INSTITUTO POLITÉCNICO DE BRAGANÇA Escola Superior Agrária

Effect of *Cryphonectria hypovirus (CHV-1)* infection on oxaloacetate acetylhydrolase (OAH) in *Cryphonectria parasitica* hypovirulent strains

Emna Belkhiria

Dissertation submited to Escola Superior Agrária de Bragança to obtain the Degree of Master in Biotechnology Engineering under the scope of the double diploma with Université Libre de Tunis

Supervised by

Maria de Lurdes Antunes Jorge
Eugénia Gouveia
Ines Ben Rejeb

Bragança
2024

Acknowledgements

I would like to express my deepest gratitude to those who have played a crucial role in my academic career and personal development.

I am deeply grateful to my supervisors, Eugénia Gouveia, Ines Ben Rejeb and especially Lurdes Jorge, for their advice, expertise and unwavering support. Your mentorship played a decisive role in the trajectory of my research.

A special mention to Valentim Coelho, whose invaluable help in the laboratory was crucial to the success of my work. Your dedication and expertise has been the cornerstone of my academic endeavors.

To my father, the man of my life. You have always set an exemplary course for me, and it's thanks to you that I am where I am today. You are my constant refuge and you always will be. I love you so much.

To my mother, the cornerstone of my character, whose encouragement and sacrifices have inspired me. Your resilience in the face of challenges and your boundless love are my constant motivation. I love you with all my heart.

Special thanks to my brother Nabil and his wife Jesse, who have supported and inspired me. Your love reminds me that I am never alone.

Deep gratitude to my childhood confidants, Wissal and Sonia, for their unwavering support and endless love. Your enduring friendship has not only added immeasurable joy to my life, but has also been the heartbeat that has fueled my courage throughout this transformative journey. I am deeply grateful to you for being a part of my life. I love you both.

A heartfelt tribute to my dear friend Maryem, whose comforting presence in a foreign land has been a lifeline, transforming unfamiliar surroundings into a place i can truly call home. I love you, Maryem.

Finally, I'd like to thank myself. For every challenge met, every obstacle overcome and every lesson learned. It's essential to recognize the resilience within us, and I appreciate the strength that has kept me going.

This thesis is not only the culmination of my academic efforts, but also a reflection of the collective love and support I have received from my family, friends, supervisors and colleagues.

May God keep you all in my life, with my sincerest THANKS.

Abstract:

Research on chestnut blight, caused by the fungus *Cryphonectria parasitica*, aims to understand and mitigate its virulence on *Castanea sativa* Mill, the main host. The use of *Cryphonectria hypovirus 1* (*CHV-1)*, known for inducing hypovirulence in the fungus, is one of the main resources of the disease biological control. Conversion of the wild *C. parasitica* by hypovirulent strains containing the virus leads to reduced fungal pathogenicity. Oxaloacetate acetylhydrolase is one of the enzymes involved in the mechanism of pathogenicity of *C. parasitica*, and its expression is known to be influenced by *CHV-1* infection.

In this study, virulent isolates of *C. parasitica* were intentionally converted to hypovirulent strains. RNA extraction was performed using two separate methods, with the purpose that the cDNA obtained was used to assess Oxaloacetate acetylhydrolase expression in isogenic converted isolates.

In the following step, we screened specific Oxaloacetate acetylhydrolase primers and two other primers to select reference genes for the execution of RT-qPCR experiments. Unfortunately, time constraints hindered the achievement of the expected final results.
In addition, a growth analysis of the isolates was performed to decipher significant differences between virulent and isogenic converted isolates.

Keywords: Chestnut blight, Hypovirulence, Biological control

Resumo:

A investigação sobre o cancro do castanheiro, causado pelo fungo *Cryphonectria parasitica*, visa compreender e mitigar a sua virulência em *Castanea sativa* Mill., o principal hospedeiro. A utilização do hipovírus *Cryphonectria* 1 (*CHV-1*), conhecido por induzir hipovirulência no fungo, é um dos principais recursos de controlo biológico da doença. A conversão de isolados selvagens de *C. parasitica* por isolados hipovirulentos contendo o vírus resulta na redução da patogenicidade do fungo. A oxaloacetato acetil-hidrolase (OAH) é uma das enzimas envolvidas no mecanismo de patogenicidade de *C. parasitica*, e a sua expressão é influenciada pela infeção por *CHV-1*.

Neste estudo, isolados virulentos de *C. parasitica* foram convertidos intencionalmente em cepas hipovirulentas. A extração de RNA foi realizada utilizando dois métodos distintos, com o objetivo de que o cDNA obtido fosse utilizado para avaliar a expressão da OAH em isolados isogénicos convertidos. Numa etapa seguinte, selecionámos primers específicos para OAH e outros dois primers para genes de referência com vista à realização de experiências de RT-qPCR. Infelizmente, as limitações de tempo impediram a obtenção dos resultados finais esperados.

Adicionalmente, foi realizada uma análise do crescimento dos isolados para identificar diferenças significativas entre isolados virulentos e isogénicos convertidos.

Palavras-chave: Cancro do castanheiro, Hipovirulência, Controle biológico,

Abbreviations

C. parasitica = Cryphonectria parasitica

CHV-1 = Cryphonectria hypovirus-1

OAH = Oxaloacetate Acetylhydrolase

PDA = Potato Dextrose Agar

IPB = Instituto Politecnico de Bragança

Vic or VCG = Vegetative Compatibility

RNA= Ribonucleic Acid

cDNA= Complementary Deoxyribonucleic Acid

GADP = Glyceraldehyde diphosphate

Rbsl_L5 = Ribosomal proteinl_ L5

PCR = Polymerase Chain Reaction

RT-qPCR = Quantitative Reverse Transcription Polymerase Chain Reaction

dNTP = Deoxynucleotide triphosphates

MgCl2 = Magnesium Chloride

List of Figures

List of Tables

Table of contents

I. Introduction

The chestnut tree (*Castanea sativa* Mill) is a majestic tree belonging to the Fagaceae family with a broad crown and rapid growth. It can be up to 35 meters high and 4 meters in diameter. Its leaves are deciduous and rich in tannins, it produces fruit that is widely eaten by humans and other animals (Conedera et al., 2004**).**

The tree-affecting disease was first detected at the New York Zoo in the early 20th century on American chestnut trees, and was dubbed "chestnut blight". Its current name was reported in 1978 (Arnold, 1980). *Cryphonectria parasitica* is an outstanding example of an introduced pathogen that has triggered devastating epidemics in native tree species (Rigling and Prospero, 2018). The disease has spread worldwide, affecting every continent (Rigling and Prospero, 2018).

Cryphonectria parasitica encountered two susceptible chestnut species *Castanea dentata* (Marsh.) Borkh. The American chestnut and *C. sativa* Mill. the European chestnut (Rigling et al., 2021).

This fungus is able to infect the tree through wounds or natural cracks in the bark, and once inside, it begins to grow and spread through the tree's vascular system. It causes cankers to form on the branches and trunk of the tree, which can lead to the death of the tree if not treated (Bragança et al., 2007). One of the main characteristics of *C. parasitica* is its ability to produce oxalic acid. Which helps the fungus to break down the lignin and cellulose of the tree (Ouni et al., 2020). This ability allows the fungus to penetrate deeper into the tissues of the tree and cause greater damage. Another characteristic of *C. parasitica* is its ability to form fruiting bodies called apothecia on the surface of cankers. These fruiting bodies produce spores which can be dispersed by wind and water and infect other nearby chestnut trees (Rigling and Prospero, 2018).

II. The Chestnut Blight

II.1 History of the Chestnut Blight

Referring to the historical records and population genetic analyses, *C. parasitica* was introduced to North America from Japan, more precisely from the island of Honshu and some other parts. The fungus was also detected in China and Korea (Dutech et al., 2012). In Europe, the first official time *C. parasitica* was identified was in 1938 in the international port in

Genoa in Italy. Genetic analyses showed additionally that the source of this introduction to Italy was North America (Rigling and Prospero, 2018). By the 1950's, chestnut disease had already spread widely in most of the main chestnut-producing regions, starting in Italy and then moving into other regions such as France, Switzerland, Slovenia and beyond. It reached Portugal in 1989 **Figure 1**. In most of these regions there is one dominant genotype probably derived from the original population in Italy, which has invaded the territory (Milgroom et al., 2008).

The importation of chestnut trees between Asia and the United States from the 1920s to the 1950s probably further facilitated the introduction of the *C. parasitica* fungus into Europe (Rigling and Prospero, 2018). **Figure 1** illustrates the spread of chestnut trees disease in European countries and the respective year of its initial observation. Many efforts to control the epidemic have been involved, such as quarantine measures, chemical treatments and the selection of resistant chestnut trees among others (Bragança et al., 2018). However, none of these methods has been able to halt the spread of the disease or even restore chestnut trees populations to their previous level of abundance. As a result, scientists have turned their attention to alternative solutions, such as biological control of the disease, more precisely the use of hypovirulence. (Milgroom and Cortesi, 2004).

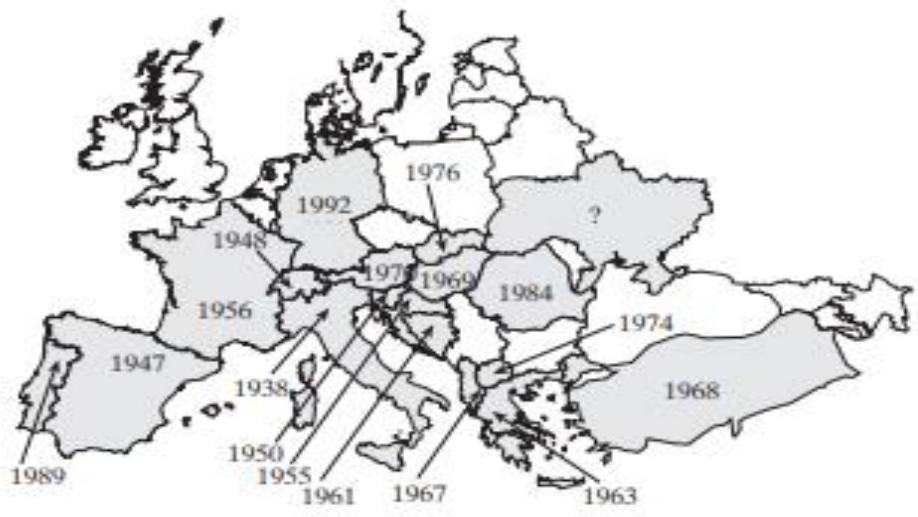

Figure 1 : The invasion of chestnut blight and its year of observation in each European country (Robin and Heiniger, 2001).

The most known efficient biological control of chestnut blight is the hypovirulence (Robin and Heiniger, 2001). This approach entails the infection of the fungus by a hypovirus. When it's infected by a hypovirus, the virulent strains of the fungus are able to decrease the disease's virulence and permit infected trees to recover and so to be saved (Robin and Heiniger, 2001). This discovery led to the development of biological control methods using hypovirulent strains of the fungus, which have been effective in reducing the impact of the disease in some areas (Arnold, 1980).

Today, endeavors to control the chestnut blight's infection continue with ongoing research into genetic engineering, hypovirulence and other methodologies for breeding and cultivating resistant chestnut trees.

II.2. Chestnut blight and its geographical distribution

The disease has spread to many parts of the world and is now considered a major problem in many countries (Bragança et al., 2007). According to the European and Mediterranean Plant Protection Organization global database **(Figure 2)**, the species is still present in some parts of the world and was eradicated in others.

In the United States for example, chestnut blight is present in many states. Although its impact is most severe in the northeast and Appalachian regions (Gilland et al., 2012).

In these regions, American chestnut trees (Castanea dentata) were once abundant and dominated the forest landscape providing valuable timber and an important food source for wildlife (Conedera et al., 2004). However, the introduction of the disease changed this dramatically. By the mid-20th century, the American chestnut had all but disappeared as the dominant tree species in the forest. Today, the epidemic continues to be a major threat to American chestnut in many areas and new outbreaks of the disease may appear even in areas where the disease was previously controlled.

In Europe, the fungal infection has been evident in many countries, including Italy, Spain, France, and Portugal. The epidemic has devastated chestnut trees (Figure 2). In Portugal, chestnut populations are highly varied in terms of structure and composition (Bragança et al., 2018). The Trás-os-Montes and Alto Douro regions constitute the most crucial chestnut hotspots in Portugal, covering approximately 85% of the chestnut-growing area (Dutech et al., 2012). The disease has been most frequently observed in high forests (Dutech et al., 2012). Notably, important areas in Portugal such as the Serra de São Mamede Natural Park and the Serra da Estrela Natural Park, which represent valuable ecosystems and ecological heritage, have also been affected by chestnut blight (Bragança et al., 2018).

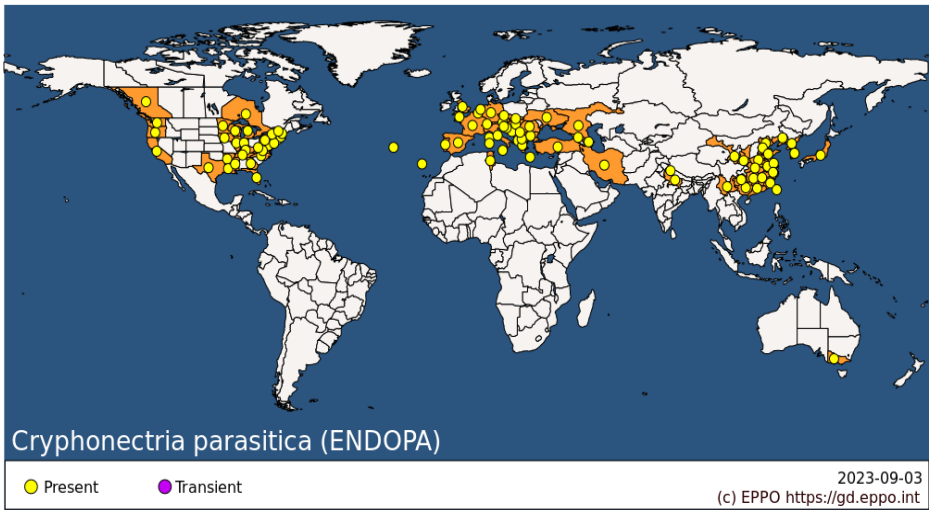

Figure 2 : Distribution of *C. parasitica* in the world (CABI/EPPO, 2023).

Referring to the EPPO Global Database, chestnut blight has also been reported in other parts of the world. Asia and China are the most affected regions, while in Australia, it has been identified with limited distribution. However, in North Africa, notably Tunisia, it has only a few occurrences.

In these regions, the disease is considered a severe threat to chestnut trees, and efforts are being made to control the spread of the disease and protect chestnut populations **(Figure 2)**. Efforts to control chestnut blight include biological control using hypovirulence therapy with *CHV-1,* breeding resistant chestnut varieties, and implementing forest management practices such as thinning and controlled burns. Additionally, monitoring programs and public education campaigns are essential in early detection and prevention.

The geographical distribution of chestnut blight is determined by several factors, including the distribution of chestnut trees, the presence of environmental conditions favorable to fungal growth, and the movement of infected material such as bark or wood (Bragança et al., 2018). To control the spread of infection, it is important to understand its geographical distribution and develop effective management strategies. These strategies include measures such as the use of disease-resistant varieties and the application of fungicides (Robin et al., 2000). However, with the advent of biological control by hypovirulence which is the subject of much in-depth research, these solutions are less crucial and this offers hope for the survival of the chestnut tree (Robin et al., 2000). Indeed, some countries in the world have managed to eradicate the disease completely such as Poland and Sweden according to the EPPO Global Database.

II.3. Chestnut blight symptoms

The aerial part of chestnut trees is the only part that can be affected by *Cryphonectria parasitica*, such as the trunk and branches (Dutech et al., 2012). The symptoms can differ depending on the infection level, advanced or not, and the fungus that infects (Rigling and Prospero, 2018). In the early stages, small circular cankers or dead areas may appear (Ouni et al., 2020). These cankers commonly have a dark color and may have a fissured appearance. The most common name referred to it is necrotic lesions or cankers (Hebard, 1984). As *C. parasitica* spreads within the tree, these cankers enlarge, and the bark may flake or peel, revealing the underlying wood. This infection can leave the tree with a weakened structure vulnerable to the environment and weather, such as wind or storms (Prospero and Rigling, 2013). Once the infection reaches an advanced stage, the nut production is diminished, leaves decrease in size, and deformation or discoloration may be produced (Hebard, 1984). This can even lead to the death of branches or even the entire tree (Bragança et al., 2018).

According to Hebard (1984), perennial cankers can form on thick branches and grow for years until the tree dies.

However, on young trunks or branches with smooth bark, the color is orange to reddish brown on the surface. In fact, the discoloration of cankers is generally less visible on older trees (Hebard, 1984). *C. parasitica* is more straightforward to detect on thin-barked trunks and branches since longitudinal cracks appear in the bark on thick trunks only after an advanced stage of infection (Rigling and Prospero, 2018). The fungus develops a typical fan of light brown hyphae. This is a clear phenotypic symptom of the infection (Prospero and Rigling, 2013). When the cambium degenerates, the bark sinks inwards, giving the trunk a hollow appearance. Leaves then wither yellow or brown, usually attached to the infected dead branches (Prospero and Rigling, 2013). This represents the most significant early symptom of *C. parasitica* infection in mature trees in the canopy. In response to infection, trees produce lignin beneath the canker (Dutech et al., 2012).

II.4. Epidemiology

Chestnut blight poses a threat to the genetic diversity of the chestnut population, as the remaining trees are often hybrids or less genetically diverse trees (Rigling and Prospero, 2018). At the start of new epidemics, the mating possibilities of *C. parasitica* are generally reduced due to the presence of a mating type that may be unique or dominant (Prospero and Rigling, 2013). Consequently, the pathogen initially reproduces mainly asexually and spreads by conidia (Caten, 1972). Sexual reproduction can also occur by self-fertilization in self-pollinating isolates when both mating types are initially present or after successive introduction of the opposite mating type (Bragança et al., 2007). Natural virulence is known to be low, which reduces the severity of damage in European chestnut (Cortesi et al., 1998; Rigling and Prospero, 2018). Temperature also contributes to the development of the disease and possibly to the reproduction of *Cryphonectria parasitica*, which can infect the tree at any stage of its life (Bragança et al., 2018). Although, it is more aggressive during the summer and autumn months, as the bark becomes softer and therefore easier to penetrate (Bragança et al., 2018). It has been shown that the disease develops at a rate of 1 mm per day in North America with an average daily temperature of 20°C (Bragança et al., 2018).

In a growth chamber experiment, symptom expansion in European chestnut was fastest at 27°C and slowed considerably below 20°C (Cortesi et al., 1998; Rigling and Prospero, 2018).

II.5. Infection mechanism

Cryphonectria parasitica the responsible agent of chestnut blight. It infects trees through natural openings in the bark as well as through wounds caused by pruning, storm damage or other factors. Once the fungus enters the tree, it begins to grow and colonize the inner bark and cambium, which are the tissue layers responsible for tree growth and nutrient transport (Rigling and Prospero, 2018). The infectious process during the disease was studied in detail using histological methods (Hebard, 1984). After spore germination, the rate and extent of hyphal formation by *C. parasitica* appears to be an important process in the spread of the cankers (Prospero and Rigling, 2013). The host tree responds to infection by lignification of the cell wall (Rigling and Prospero, 2018). However, hyphae can invade and damage the lignified regions of host cells. Only a fully developed damaged epidermis prevents further integration of the hyphal compartment (Rigling and Prospero, 2018). As the hyphal compartment progresses, host cells are killed by toxins and cell-wall degrading enzymes resulting in continued inhibition of wound periderm formation (Rigling and Prospero, 2018).

A metabolite probably involved in this process is oxalic acid, which is secreted by *C. parasitica* and causes toxic effects on host cells, thus promoting cell wall degradation (Rigling and Prospero, 2018).

Through specific genetic mutations, many virulence factors have been identified in *C. parasitica*, such as confirmation of the role of oxalic acid or G-protein signaling, kexin-like proteases involved in protein secretion, the homologous transcription factor Ste12, protein kinase 2 (CK2)-mediated signaling and the apoptotic protein inhibitor (CpBir1) (Chun et al., 2020, Rigling and Prospero, 2018).

II.6. Vegetative compatibility

Vegetative compatibility is a mechanism that allows certain strains of a fungus to recognize and physically interact with each other. In the case of *C. parasitica*, vegetative compatibility is determined by a group of genes called vegetative compatibility (*vic*) genes (Prospero and Rigling, 2013).

The various strains of *C. parasitica* have distinct combinations of *vic* genes and a genetically diverse aspect of mycelium is produced if these *vic* types are compatible. The strains can then physically interact with each other and this process is known as hyphal fusion, which allows the exchange of genetic information and, thus, the creation of new strains with various characteristics, such as increased virulence or resistance to new fungicides (Caten, 1972). The

survival of *C. parasitica* depends on this compatibility since the fungus needs this compatibility to interact (Cortesi et al., 1998). This process of genetic exchange can also lead to the emergence of new pathogenic strains (Cortesi et al., 1998). *Cryphonectria parasitica* uses this vegetative incompatibility to prevent cytoplasmic infection (Bragança et al., 2007).
Currently, there are six independent *vic* loci of vegetative incompatibility in *Cryphonectria parasitica*, each composed of two alleles (Rigling and Prospero, 2018). For *C. parasitica* isolates to be compatible, these alleles must be the same at all vegetative incompatibility loci. This compatibility is evident in agar co-culture by the fusion of compatible strains. Otherwise, incompatible isolates develop a barrier along the contact zone, as shown in **Figure 3** (Rigling et al., 2021).

Figure 3 : Example of an incompatible strain (Rigling et al. 2021).

This barrier line is the result of programmed cell death (apoptosis) triggers when incompatible cells anastomose. The six genetically defined *vic loci* have also been characterized at the molecular scale (Robin et al., 2000).

The research revealed that complex allelic and non-allelic interactions can occur at these *vic loci* (Choi et al., 2012). Based on the molecular characterization of these *loci*, a polymerase chain reaction (PCR)-based method has been developed to identify each currently known *vic* genotype.
The identification of *vic* genotypes is better when the populations are less diverse in *vic* types (Cortesi et al., 1998). No other fungus has such comprehensive information available in terms of *vic* genotypes (Cortesi et al., 2001). Thirty-one *vic* types from Italy and Switzerland were

discovered among samples of over 1,000 isolates by Cortesi and Milgroom (1998). The limited diversity in vic types may be attributed to at least five polymorphic vic loci, assuming the existence of two alleles for each locus. The regulation of vegetative incompatibility in *C. parasitica* is believed to be controlled by allelic interactions at five to seven *vic loci* (Anagnostakis, 1986). Anagnostakis (1998) identified two *vic loci*, *vic1* and *vic2*. Three additional *loci*, *vic3*, *vic4*, and *vic5* were later identified by Cortesi and Milgroom (1998), who successfully assigned all 31 European vic genotypic types (EU-1 to EU-31) discovered in the field to specific *vic* genotypes.

III. *Cryphonectria parasitica*

III.1. Characterization

Cryphonectria parasitica is a fungus known to have a unique appearance when grown. Under the microscope, the fungus appears as a hyphal growth consisting of long, thin, and branched filaments (Özkilinç, 2018). The hyphae are usually white or pale yellow and have a smooth, shiny surface (Özkilinç, 2018). The fungus also forms characteristic fruiting bodies called apothecia (Rigling and Prospero, 2018), which are dark brown or black. These fruiting bodies produce spores that can be transported by wind and water and infect other chestnut trees. Additionally, *C. parasitica* produces a survival structure that can last dormant in the environment for long periods until conditions are favorable for its growth. Known as a chlamydospore and which is characterized by a thick wall. The latter also plays a primordial role in the survival of the fungus since this mechanism helps to infect new trees (Özkilinç, 2018).

III.2. Hypovirulence by *CHV-1*

III.2.1 The hypovirus *CHV-1*

Hypoviruses are positive-strand RNA viruses that reside in the cytoplasm membrane vesicles of fungal hosts (Fahima et al., 1993). They lack envelope proteins and are associated with host-derived membrane vesicles (Fahima et al., 1993). Hypoviruses have traditionally been detected in fungal mycelium by extraction of double-stranded RNA representing the replicative form of the virus (Rigling and Prospero, 2018).

Cryphonectria parasitica features four extensively characterized species, specifically *Cryphonectria Hypovirus 1* (*CHV-1*), *CHV-2*, *CHV-3*, and *CHV-4* (Rigling and Prospero,

2018). Among these, *CHV-1* is the most thoroughly studied and is utilized in Europe as a biological control agent against chestnut blight (Rigling and Prospero, 2018). *CHV-1* induces a low pathogenic phenotype in *C. parasitica*, leading to a reduction in the pathogen's growth and its ability to sporulate (Ouni et al., 2020). According to the studies, there is no clear cycle that *CHV-1* follows to infect its host (Rigling and Prospero, 2018).

Indeed, the virus is transmitted by cytoplasmic exchanges carried out by the fungus itself, which is explained by a fusion of hyphae controlled by the vegetative incompatibility genes or *vic* (Gobbin et al., 2003).

However, despite the defense mechanism used by this fungus to protect itself, *CHV-1* spreads more efficiently and quickly, between 4 and 6 hours (Rigling and Prospero, 2018). This is due to the inability of *CHV-1* -infected hosts to mate sexually, as infection with the virus suppresses allelic recombination at the *vic loci* and therefore increases the rate of spread, not to mention the ability of the virus double-stranded RNA to spread even if the *vic* genes are not the same (Rigling and Prospero, 2018).

III.2.2 *CHV-1* and *Cryphonectria parasitica* interaction

Strains infected with *CHV-1* also have other phenotypic manifestations such as decreased pigmentation and sporulation (Gobbin et al., 2003). It is *CHV-1* that causes these phenotypic changes interacting with fungal signaling pathways. Indeed, these hypoviral effects on cell signaling were noted in *C. parasitica* after culture and exposure on PDA (Gobbin et al., 2003).

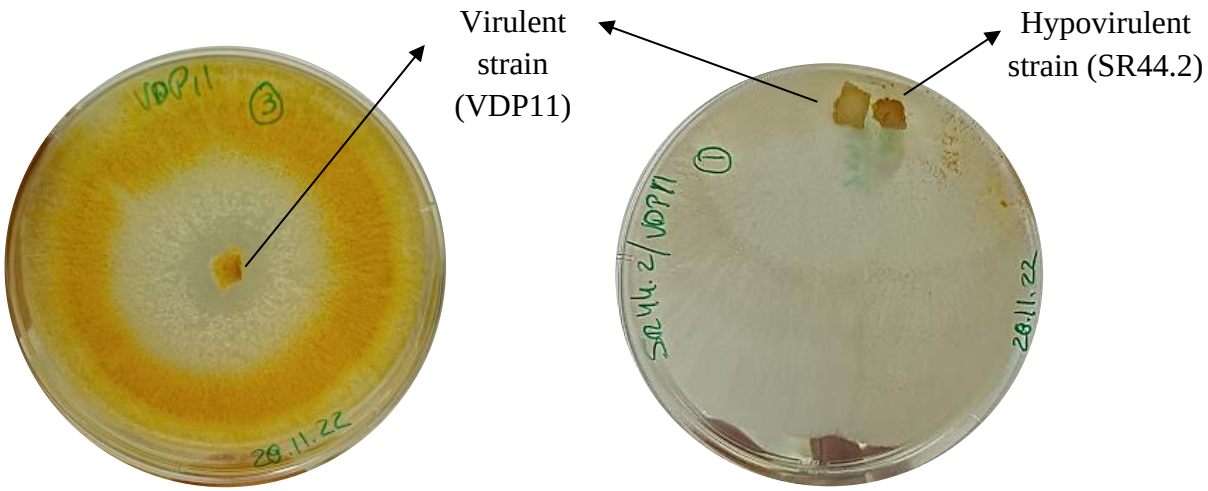

Figure 4 : The phenotypical manifestation of a virulent strain of *C. parasitica* when it's placed on PDA with a hypovirulent strain (Chun et al, 2020).

Without hypovirus, cultures generally exhibit orange pigmentation and abundant asexual sporulation. On the other hand, cultures infected with hypovirus show very low or even non-existent sporulation, as illustrated in **Figure 4**. These signaling processes also play a crucial role in the infection mechanisms. Additionally, research indicates that RNA silencing constitutes a novel defense mechanism the fungal host uses against viral infections (Segers et al., 2007). Several studies have observed considerable variability in the hypoviral virulence of *CHV-1*, even within local populations (Bryner et al., 2012; Peever et al., 2000). Genome comparison and mutational analysis of low and high-virulence *CHV-1* strains have revealed specific viral genome regions associated with these mutations (Chen et al., 2010).

Furthermore, one study found a positive association between hypovirus virulence and hypovirus transmission across the vegetative incompatibility barrier (Bryner et al., 2012). The reason for this association is unknown. However, the higher pathogenicity of hypoviruses may compensate for their debilitating effects on their fungal hosts and may explain why pathogenic hypoviruses are present in different populations of *C. parasitica* (Bryner et al., 2012). Hypovirulence affects not only *C. parasitica* phenotypically but also genetically (Cortesi and Milgroom, 1998). As mentioned earlier, the pathogen infects the tree via enzymes that destroy the tree's plant cells. *CHV-1* also affects the expression of these enzymes. Several studies have been carried out to investigate this effect.

For example, Savino S (2021) showed an increase in the production of the enzymes laccase and esterase by hypovirulent *C. parasitica* compared with a virulent strain (Savino et al.,

2021). The latter even suggested the feasibility of large-scale enzyme production of industrial interest, given the extent of enzyme production by the strain when hypovirulent (Savino et al., 2021). Another study also demonstrated that hypovirulence in *C. parasitica* can produce a new extracellular laccase following deletion of the Lac1 gene, which codes for its expression (Kim, 1995).

Ecological factors may also favor infection of *C. parasitica* by *CHV-1*, which has the attractive characteristic of primarily affecting parasites rather than the saprophytic growth of the host organism. In its natural environment, hypovirus-infected strains can survive and reproduce asexually on dead chestnut bark, thus serving as a reservoir of hypovirus inoculum (Rigling and Prospero, 2018).

IV. Oxidative enzymes degrading the cell-wall components

IV.1 Components of the cell wall

As shown in **Figure 5**, plant cell walls comprise three main components: cellulose, hemicellulose, and lignin (Bidlack, 1992). Other substances, such as protein and pectin, may also be present in lignocellulosic residues (Bidlack, 1992).

Cellulose is a linear biopolymer consisting of glucose units linked by β-1,4-glycosidic bonds. This complex carbohydrate is the main component of plant materials. As a vital factor in plant growth and morphogenesis, cellulose synthesis plays a central role in forming plant cells and tissues, providing structural support and integrity to cell walls (Lei et al., 2012).

In contrast to cellulose, hemicellulose is a heterogeneous polymer consisting of pentoses, hexoses, and sugar acids (Heinze, 2005). Lignin, the most abundant naturally occurring aromatic polymer, consists of phenylpropanoid units called monolignols or lignin precursors. These units are linked together by carbon-carbon and carbon-oxygen bonds, with varying degrees of methoxylation (Heinze, 2005).

Lignin is mainly found in the primary cell wall, giving its rigidity and acting as an adhesive that holds the cells together. It is crucial in protecting the polysaccharides against microbial degradation (Argyropoulos and Menachem, 1997).

By combining cellulose and hemicellulose, lignin acts as a barrier and prevents enzymes from reaching the inner structure of lignocellulose (Argyropoulos and Menachem, 1997). Furthermore, as a hydrophobic polymer, lignin is a barrier against water penetration (Argyropoulos and Menachem, 1997).

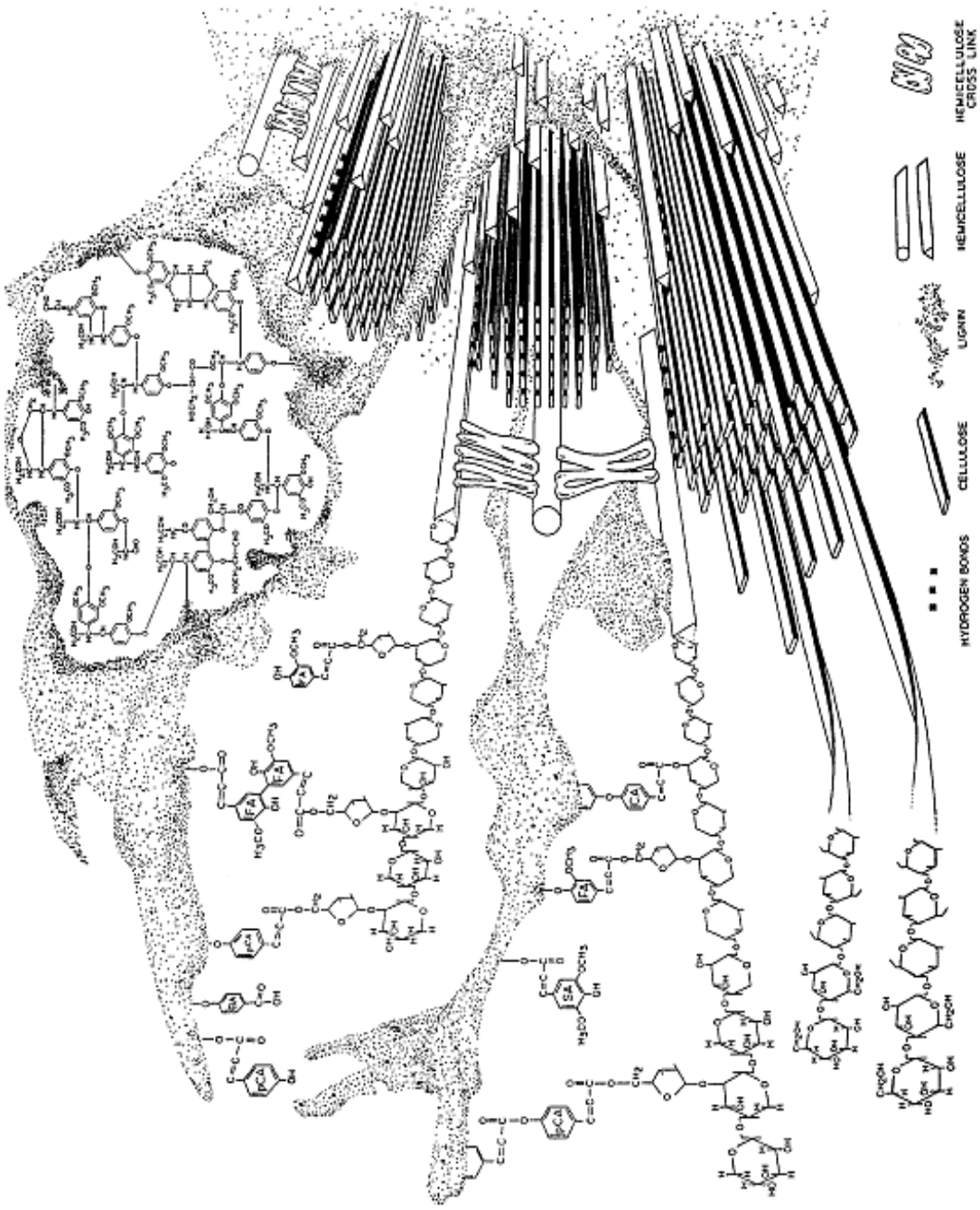

Figure 5 : Main components of the secondary plants cell wall (Bidlak, 1992).

IV.2. Enzymes involved in the cell-wall degradation

Degradation by oxidizing compounds bound to lignin. They are glycoproteins that occur in extracellular and intracellular forms and often form multimeric complexes. Laccases is belonging to the superfamily of multicopper oxidases MCOs and can oxidize a wide range of compounds, making them "ideal green" catalysts (Galhaup and Haltrich, 2001). Lignin peroxidase (LiP) plays a vital role in the biodegradation of lignin, a major component of plant cell walls. LiP (EC 1.11.1.14) can oxidize aromatic compounds that have a redox potential of more than 1.4 V (NHE) by abstracting a single electron. However, the exact details of the redox mechanism involved in this process still need to be better understood (Piontek et al., 2001).

Manganese peroxidase (MnP) is an enzyme involved in degrading phenolic lignin components. Certain fungi produce it and oxidize Mn2+ to Mn3+ using H2O2 as an electron acceptor. The catalytic cycle implicates the formation of an iron II peroxide complex, the release of two electrons, and a reduction of MnP compound I to compound II by Mn2+, resulting in Mn3+ as a potent oxidizing agent for the one-electron oxidation of phenolic structures (Swe, 2011).

IV.2.1. Oxaloacetate acetylhydrolase

IV.2.1.1. Mode of action

Oxalate secretion is usually known to be associated with fungal pathogenesis (Han et al., 2007). After invading the tree bark by splitting the cells, *C. parasitica* prevents the tree from repairing the wound by producing cell wall degrading enzymes as well as metabolites such as oxalic acid, which are toxic to the host cells and contribute to their wall degradation (Bryner et al., 2012; Prospero and Rigling, 2013). Inactivation of the gene encoding the oxalic acid-producing enzyme confirmed its role in pathogenesis (Chen et al., 2010).

Oxaloacetate acetylhydrolase (OAH) is an essential enzyme in fungal metabolism and mode of action (Han et al., 2007). This enzyme catalyzes the hydrolysis of oxaloacetate to oxalic acid and acetate, as shown in **Figure 6**.

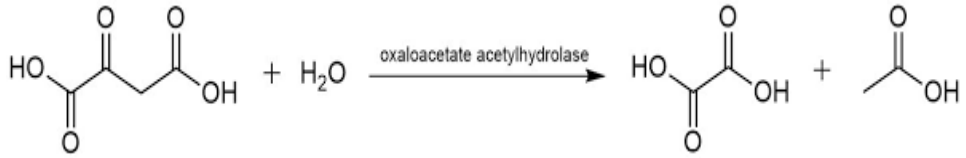

Figure 6 : The enzyme oxaloacetate acetylhydrolase catalysis (Ouni et al, 2020).

The virulence mechanism in these fungi is thought to be due to acidification that triggers lignocellulose degradation that reduces host tissue viability in favor of pathogen proliferation and induces calcium oxalate crystallization (Han et al., 2007).

The role of oxaloacetate acetylhydrolase and oxalic acid production in fungal pathogenesis is complex and multifaceted. While the mechanisms underlying these processes are still being studied, a better understanding of the role of oxalate metabolism in fungal virulence could provide new insights into the development of effective treatments for fungal diseases.

IV.2.1.2.The OAH characterization

Oxaloacetate acetylhydrolase or OAH is an enzyme that is belonging to the phosphoenolpyruvate mutase or PEPM, isocitrate lyase superfamily. Which includes members that act on α-oxycarboxylate substrates by cleaving or forming C-C or P-C bonds (Chen et al., 2010). These members are all oligomeric proteins primarily tetramers (Giangrande et al., 1975). The active site of OAH is located at the C-terminal side of the β-barrel. In most, but not all, phosphoenolpyruvate mutase isocitrate lyase superfamily members have a mobile loop that controls access to the active site. When the substrate binds, this mobile loop closes to isolate the catalytic site from the solvent (Chen et al., 2010). To be active, all the members of the superfamily require Mg2+ or Mn2+. These two metals mediate the interactions between the protein and the substrate. These interactions are essential for the catalysis of the enzymatic reaction (Chen et al., 2010; Ouni et al., 2020).

V. Objectives

- Convert 5 virulent strains of *Cryphonectria parasitica* (EU-11, EU-66) to hypovirulent by the *CHV-1* hypovirus.
- Extraction of total RNA from both virulent strains and virulent ones in interaction with *CHV-1* to confirm the conversion to hypovirulent of the wild strains of *C. parasitica*.
- Experiment the annealing of the primers designed, in aim to evaluate the effect of the hypovirulence on oxaloacetate acetylhydrolase expression.

VI. Materials and Methods

VI.1. Strains used in this study and conversion

The table below lists the designation and vegetative incompatibility genotype *(vic)* of all virulent and hypovirulent isolates used in this work.

Table 1 : The *vic* type and the designation of each sample used in this study.

Type of strain	Designation	Vegetative incompatibility genotype	Site
Virulent	VDP11	EU66	
	Cast 13	EU11	Castrelos (Bragança)
	Cast 26	EU11	Castrelos (Bragança)
	Curopos 15	EU11	
	VBC 02	EU11	
Hypovirulent	Serra 05	EU11	
	RBB111	EU11	Rio Bom (Valpaços)
	SR44.2	EU11	Sergude (Felgueiras)

The conversion process involved placing virulent and hypovirulent isolates of *C. parasitica* approximately 5 mm apart in a Petri dish containing PDA, as illustrated in **Figure 7**. The converted strains could be distinguished from the original virulent strains since they develop white mycelia characteristic of hypovirulent strains. A piece of mycelium from each converted strain was removed and transferred to a new PDA Petri dish for maintenance.

The conversion method	Picture taken at the IPB laboratory
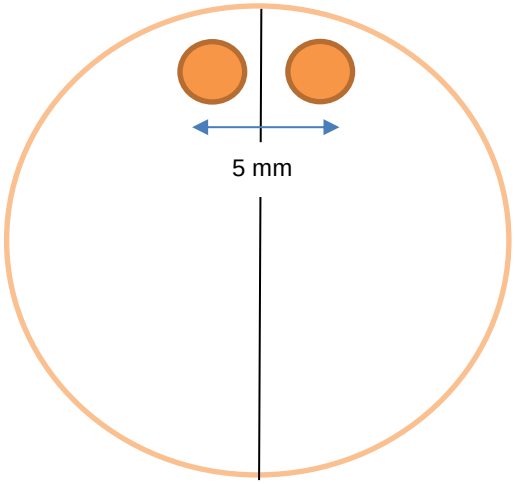	

Figure 7 : Demonstration of the conversion method used in this study.

In this case, hypovirulence was transmitted to a virulent isolate using a characterized hypovirulent isolate of *C. parasitica* carrying *CHV-1* as a donor. This conversion was performed through hyphal anastomosis, following the method of Cortesi et al. (1998). Isolates were paired in 90mm diameter Petri dishes. The plate area was divided into two, and small square sections of agar-mycelium from the isolates were placed 2.5 mm apart from the medium line. Virulent isolate on one side and the hypovirulent one on the other **(Figure 7)**. For each combination, three replicates were made to evaluate the conversion capacity. Plates were then placed at 25 ± 1°C in the dark for 14 days, followed by seven days of exposure to natural light to determine if the virulent isolate had been converted.

Mycelium from each converted strain was transferred to fresh PDA medium at 20ºC, and the growth was measured by a measuring ruler over the days. Later, the plates were maintained at 6-8°C.

The converted strains can also be transferred to a liquid media for better extraction. The culture of malt extract and peptone with a pH = 5.4 ±2 was incubated with a small agitation of 100 rpm at 25°C in the dark for seven days. The **Figure 8** was captured after the incubation at the laboratories of IPB.

Figure 8 : Example of a *C. parasitica* culture in liquid malt extract media after incubation.

VI.2.The morphological characterization

Following the cultivation process, each Petri dish underwent observation. The diameter of the growth was measured, and the color of the mycelium was duly recorded. This procedure was iterated with each culture refreshment on new PDA. The observed color aided in formulating a hypothesis regarding the potential transfer of the virus from the hypovirulent to the virulent strain. Subsequently, confirmation of this hypothesis was sought through the detection of *CHV-1* RNA using PCR.

Statistical analyses of mycelial growth were carried out using one-way analysis of variance (one-way ANOVA) followed by a post hoc LSD and Tuckey test using Statistica 12 software (StatSoft Inc., Tulsa, OK).

VI.3.The Conversion confirmation

To confirm the conversion, total RNA was extracted using two methods and *CHV-1* RNA was amplified by PCR. Results were subsequently confirmed by electrophoresis.

The two methods of extraction used starts by the freeze-drying of the mycelia with liquid nitrogen.

VI.3.1 The extraction of RNA by the TRIZOL method

The RNA was extracted with the TRIZOL method. The steps of the extraction are illustrated in **Figure 9** and the details can be found in the **Appendix 1**. The mycelium was macerated with liquid nitrogen and transferred to an Eppendorf tube where TRIZOL was added. Chloroform was added to separate the organic and aqueous phases, facilitating the purification of the RNA. After adding a high salt solution to the supernatant, the addition of isopropanol caused pellet formation, which was then collected by centrifugation and finally purified with ice-cold DEPC-treated 75% ethanol. The purified RNA was kept in DEPC-treated water to ensure the absence of RNases.

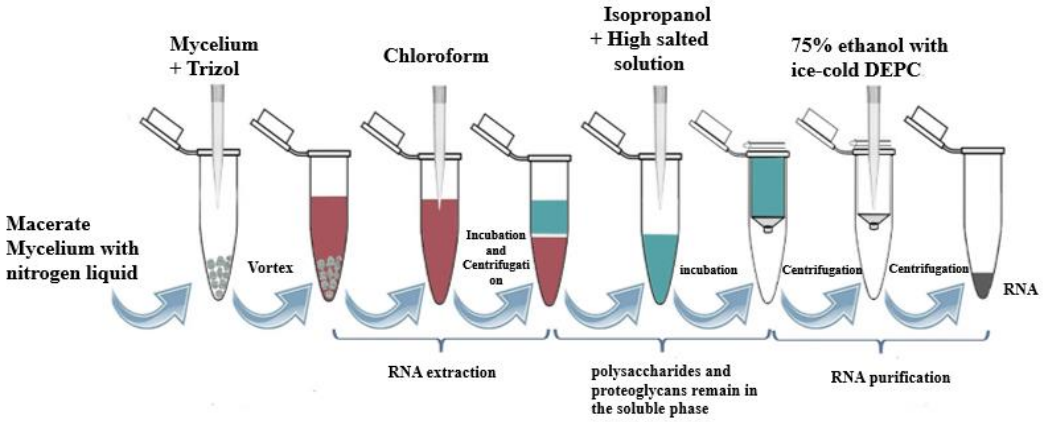

Figure 9 : RNA extraction by Trizol method.

The centrifugation process resulted in a discernible pellet in the Eppendorf tube, clearly visible to the naked eye, as illustrated in the **Figure 10** below. This pellet represents the concentrated and purified RNA obtained during the extraction procedure

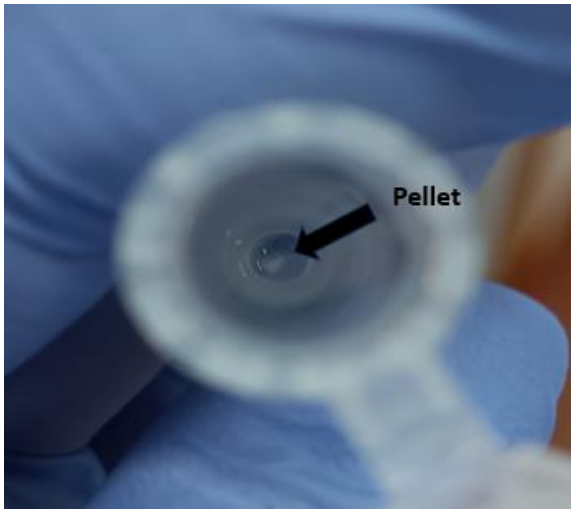

Figure 10: Pellet formation after centrifugation in RNA extraction by Trizol method.

VI.3.2.The RNA extraction protocol

The plant Fungal Total RNA Purification Kit (Norgen Biotek Corp) in **Appendix 2** was used for total RNA extraction.

As illustrated in the **Figure 11**, mycelium of the sample was initially treated with lysis buffer, followed by vortexing and centrifugation. The supernatant was transferred to a new tube, and the same ethanol volume was added. The solution was then transferred to a centrifugation. The supernatant was taken, and the column was washed before repeating the process. After a final wash, the dry column was centrifuged. The column was then transferred to a new tube, elution buffer was added, and the mixture was centrifuged. Finally, the eluted total RNA extracted was stored at -4°C if for two days and -80°C if for a longer duration.

Figure 11 : Plant-Fungal Total RNA Purification kit protocol steps.

To verify the results, electrophoresis was conducted using a 1.0% agarose gel in 1X TBE buffer at 80V for one hour. 3µL of the respective sample was introduced, supplemented with 1µL of blue dye **Appendix 3**, and 2µL of ultra-pure water. A 100 bp marker was used as reference.

VI.3.3.The *CHV-1* identification

The protocol was conducted in three steps in **Appendix 2**, diluting the total RNA and then synthesizing cDNA.

For the identification of the *CHV-1* virus, the previously extracted RNA underwent centrifugation. Subsequently, a dilution was prepared by combining Total RNA with Nuclease-free Water in microtubes. This mixture was briefly vortexed before being subjected to a 2-minute incubation at 100 °C in the T100 Thermal Cycler (Bio-Rad).

For the next step, involving the generation of complementary DNA (cDNA), separate tubes were prepared with the following components (Norgen Biotek Corp): 4 µl of 5x reaction mix, 2 µl of Maxima Engyne mix, and 14 µl of the RNA dilution. Each tube was vortexed for 3 seconds. PCR was then performed to obtain cDNA using **(Figure 12)**.

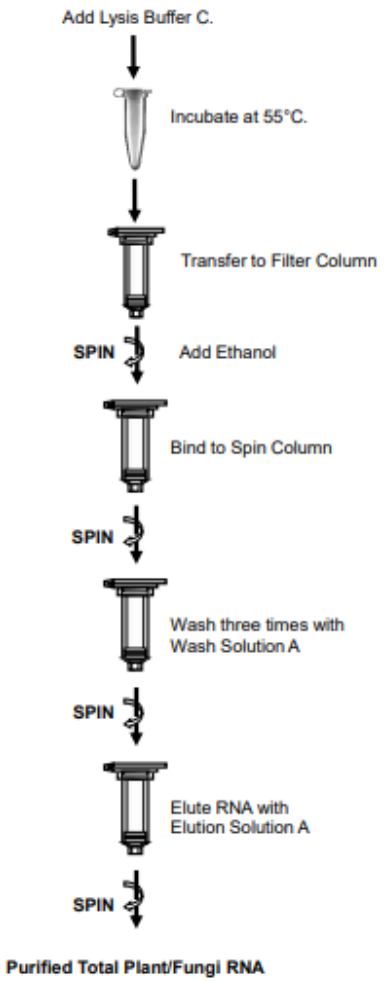

Figure 12 : Protocol performed by the T100 Thermal Cycler.

- **PCR amplification of the ORF region**

Performing a PCR to visualize the virus genome, amplifying the ORF A and ORF B regions of the genome using the primer pairs.

For the **ORF A** region (Gobbin et al., 2003) :

- Reverse Primer EP721-4 Rev (5´- GGAAGTCGGACATGCCCTG - 3´)
- Forward Primer hvep1F for (5`- TGACACGGAAGCTGAGTGTC - 3´)

For the **ORF B** region (Feau et al., 2014) :

- Forward Primer orfB-12aF for (5´- AGACCTCAATCGGGTCTCCCT - 3´)
- Reverse Primer orfB-12aR Rev (5´- TTCAACCACACGACGAGTTCG - 3´)

The PCR was done by a T100 Thermal Cycler Bio-Rad model with an initial denaturation at 94ºC for two minutes; after that, 34 cycles of denaturation were performed at 94ºC for 60

seconds. The annealing was at 55ºC of the two primers for 90 seconds followed by the extension step at 72ºC for 120 seconds, finalized by an extension step at 72ºC for 8 minutes. This process was concluded with an indefinite hold at 10ºC. A negative control was also incorporated into each PCR to identify potential contamination.

- **Visualization of PCR products**

Electrophoresis was done on a 1.5% agarose gel in TBE buffer (60 mL TBE, 0.9g agarose, 1.2 µL gel red) at 80 V using 4 µl sample, 1 µL blue dye, and 1 µL of nuclease-free water. A 100 bp DNA Marker from Bioron served as the molecular marker in this experimental procedure.

VI.4. Quantification of the RNA extracted

Quantifying nucleic acid solutions was achieved through various methods. In the case of a pure solution, a VWR® UV-3100PC, UV/Visible spectrophotometer was utilized to gauge the extent of ultraviolet radiation absorption by the nucleic acid bases. Alternatively, DNA quantification was performed by measuring the amount of ultraviolet radiation absorbed by the bases.

In this study, the spectrophotometric method was performed using H2O as a blank, and each sample was placed in a 700µL quartz cuvette. For a 1 cm pathlength, the optical density at 260 nm (OD260) equaled 1.0 for a 40 µg/mL solution of RNA. The OD260/OD280 ratio was calculated for an indication of RNA purity, knowing that pure RNA has an OD260/OD280 ratio of ~2.0. The RNA concentration (mg/mL) was calculated as shown in the formula below.

[RNA] = 40µg/mL x OD260 x dilution factor

The calculation of RNA concentration helped us estimate the amount of RNA extracted, providing crucial information for determining the volume of the sample needed to synthesize the cDNA.

VI.5. cDNA synthesis

For cDNA synthesis, the iScript Select cDNA Synthesis kit from Bio-Rad was employed in **Appendix 4**. This kit includes iScript Reverse Transcriptase, a 5x reaction buffer with dNTPs, magnesium chloride, and stabilizers.

It also contains a set of oligo(dT) primers, an enhancer solution required in reactions using gene-specific primers, and nuclease-free water.

VI.6. Annealing of the primers

For a comprehensive investigation of OAH expression in both virulent and in converted hypovirulent strains, the methodology would have been to execute a Reverse Transcription quantitative Polymerase Chain Reaction (RT-qPCR). Such an approach is advantageous for its ability to provide precise quantification of gene expression. It allows for a nuanced understanding of potential variations in OAH expression among different strains.

Unfortunately, given the time limitations inherent in this study, the implementation of RT-qPCR was not deemed practical. Primers were designed by Bio-Edit and tested by PCR on wild-type and converted hypovirulent strains, laying the foundations for further exploration in subsequent research projects.

For the subsequent phases of this study, three primers were meticulously. The genomic data of the gene encoding oxaloacetate acetylhydrolase were obtained in FASTA format from the National Center for Biotechnology Information (NCBI) GenBank database (GU932672.1). And primers for the amplification were designed using Prime3plus software (version: 3.3.0).

Two other primers that were intended to serve as reference genes for studying OAH expression were picked also. One coding for glyceraldehyde biphosphate and the second for Rbsl_L5. DFS-Taq DNA polymerase protocol was performed to experiment the annealing of these three primers **Appendix 6**.

The PCR is performed following the conditions detailed in the **Table 2** on 25µL samples. These parameters can be optimized according to the result of the electrophoresis. The primers used for this work are listed in the **Table 3** below.

Table 2 : Thermocycler protocol used.

Step	Time	Temperature
Initial denaturation	3 minutes	94°C
37 Cycles		
Denaturation	30 seconds	94°C
Annealing	20 seconds	55 – 68°C
Extension	30 seconds	72°C
Final extension	5 minutes	72°C
Hold	∞	4°C

Table 3 : Primers used to verify OAH expression.

Gene	Primer's design
OAH	OAH1 FW 5'-GTCTTGGCCAGCCTGATCTT-3' OAH1 RV 5'-AAGATCAGGCTGGCCAAGAC-3'
GADP	GADP FW 5'-AGGTCGGCATCAACGGATTT-3' GADP RV 5'-TGAGCATGTAGGCAGCGTAG-3'
Rbs1_L5	Rbsl_L5 FW 5'-AGCACTTCAAGGGTGTCGAG-3' Rbsl_L5 RV 5'-GCCAGACCGACATCAAGGAA-3'

Once the PCR has been performed, electrophoresis was carried out on a 2% agarose gel in TBE buffer at 70 V using 3 µL of sample, 1 µL of blue dye, and 2 µL of nuclease-free water. A 100 bp DNA marker was utilized for reference.

VII. Results and Discussion

VII.1. Conversion of the virulent strains

VII.1.1. Morphological characterization

Well before converting the virulent strains, it is first necessary to put each strain in PDA culture to observe the growth of each culture individually in millimeters.

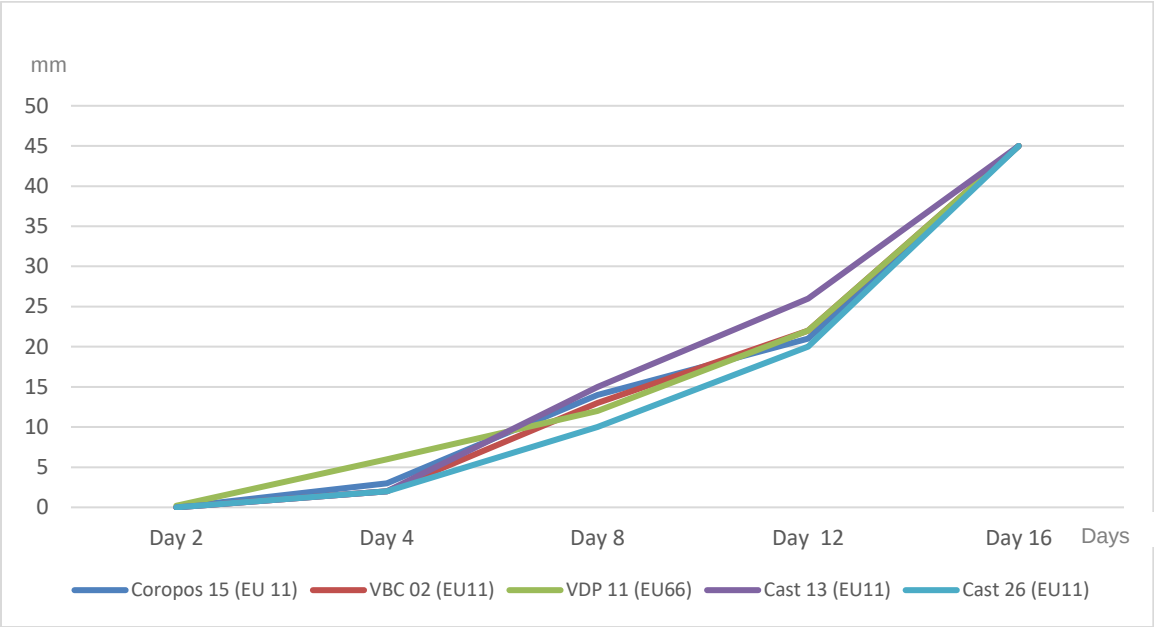

Figure 13 : Growth evolution in millimeters of the virulent strains used in this study.

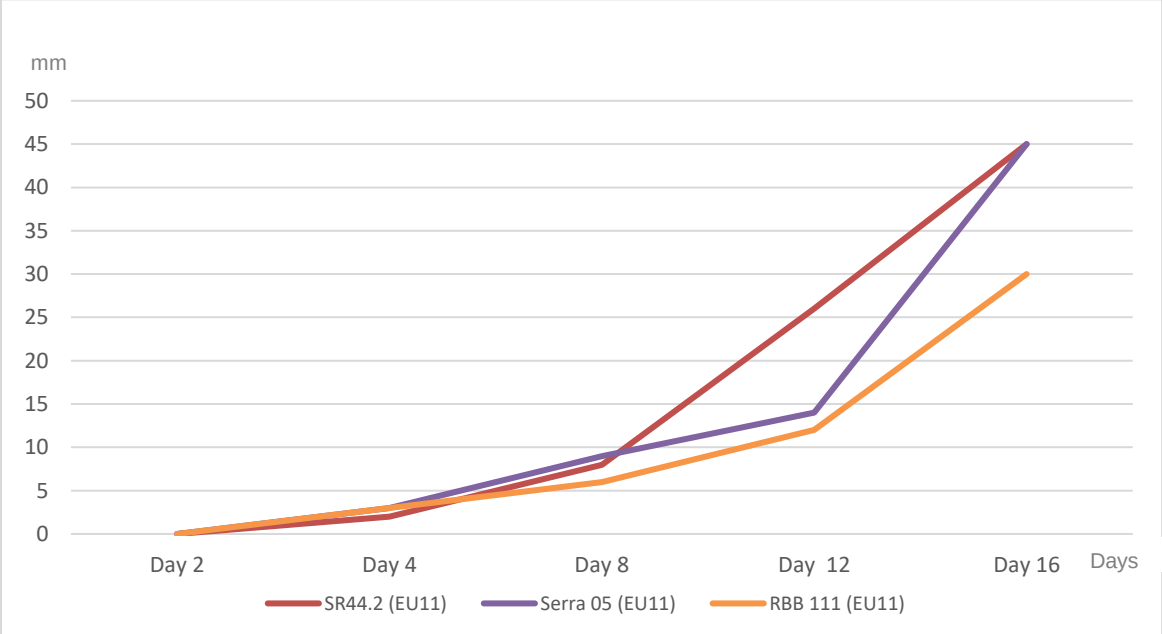

Figure 14 : Growth evolution in millimeters of the hypovirulent strains used in this study.

Figures 13 and 14 illustrate the growth of the virulent and hypovirulent strains by measuring growth over time. Comparing the two types of strains, we can observe that the wild strains grew a few millimeters more than the hypovirulent strains. However, this only concerns this work and this difference is not considered significant. In general, it has been shown that hypovirulent strains usually grow in the same way and at the same speed as wild-type strains (Rigling et al., 2018). On PDA virulent strains show orange pigmentation and a few spores. The hypovirulent strains on the other hand, show a white mycelium with no orange coloration or pigmentation. SR44.2 seems to be the fastest-growing strain compared with the other two hypovirulent strains, and in particular RBB111, which seems to be the slowest-growing.

The culture of each individual strain allows us to observe and record the behavior of each strain and to better understand the outcome and phenotypic manifestation of each combination.

A hypothesis has been established that all the virulent strains were converted successfully. In fact, the appearance of white mycelium as well as the clear decrease in pigmentation allows us to deduce the conversion of wild strains into hypovirulent ones by the presence of the *CHV-1* virus, knowing that these phenotypic manifestations are part of the symptoms of *C. parasitica* infection by the *CHV-1* virus.

In **Figure 15**, the growth of each virulent strain compared with its three different isogenic converted ones is represented. It can be supposed that hypovirulence has a somewhat attenuating effect on the growth of *C. parasitica*. The curves in black are the curves representing the virulent strains. As shown, the fungus, whether virulent or hypovirulent, will always grow, and this differs from one hypovirulent strain to another. However, this difference can be not significant.

The virulent strains combined with the hypovirulent strain SR44.2 (purple curve in **Figure 15**). These strains grew at a very similar rate to the virulent ones, even if this hypovirulence was clearly observable on Petri dishes, as the strains developed a white mycelium with no orange pigmentation.

Unlike the strain SR44.2, the other two in interaction with virulent *C. parasitica* showed briefly a decrease in growth rate following hypovirulence (the two red and blue curves in **Figure 15**). This decrease is more noticeable in strains converted with RBB111, which showed more of the phenotypic manifestations of hypovirulence.

We can therefore deduce that RBB111 has a higher phenotypical effect on *C. parasitica* than the other two hypovirulent strains, and this can be observed on PDA.

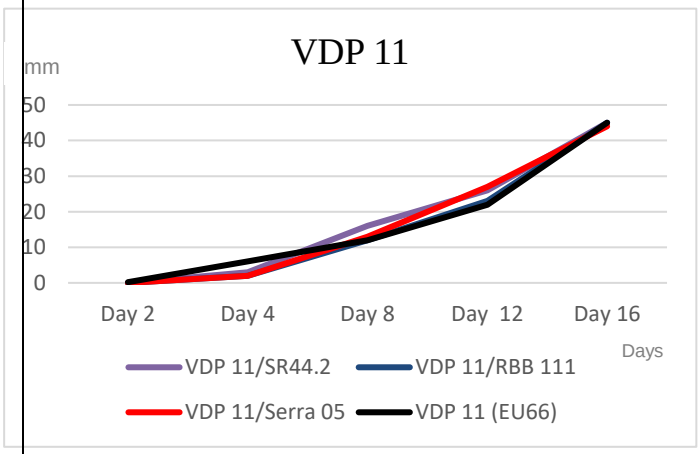

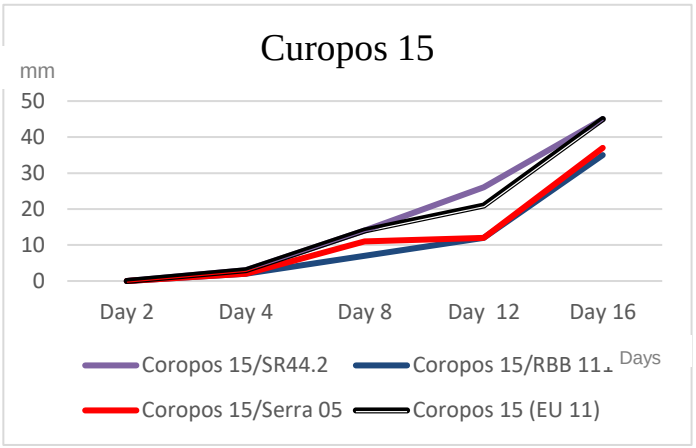

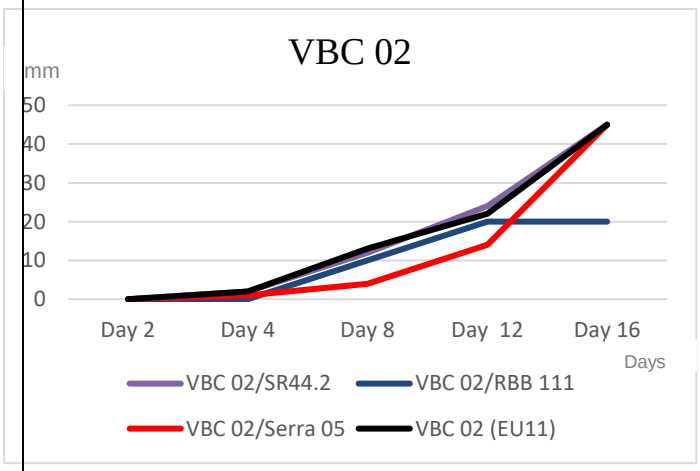

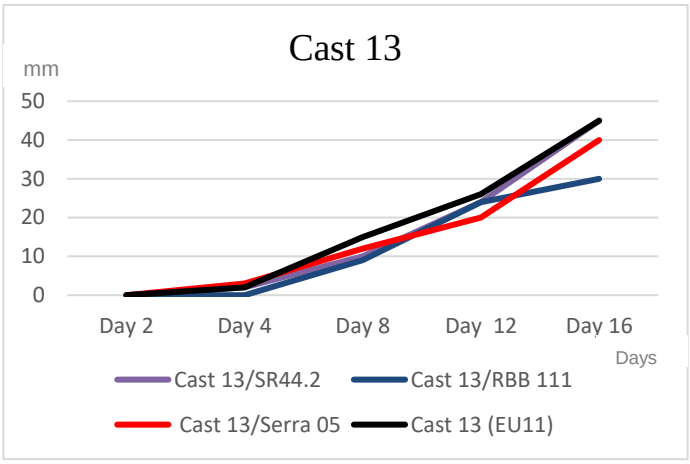

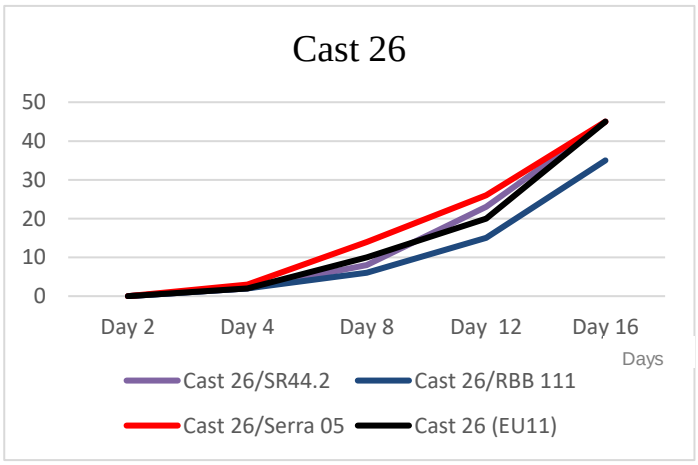

Figure 15 : The growth of each virulent strain compared with the virulent crossed with each *CHV-1* donor strain.

mm

The table below shows mycelial growth in millimetres on PDA after incubation of the virulent isolates (VDP11, Cast13, Cast26, Curopos15 and VBC02) and the latter when converted by SR44.2, RBB111 and Serra05. Different letters in the line mean significant differences ($\alpha<0.05$).

Table 4 : Effect of conversion factors on mycelial growth of virulent isolates: comparative analysis of the effect of SR44.2, RBB111, and Serra05.

		Converted by		
	No Converted (mm)	SR44.2 (mm)	RBB 111 (mm)	Serra 05 (mm)
VDP11	45.00±0.00 a	45.00±0.00 a	45.00±0.00 a	44.00±1.73 a
Cast13	45.00±0.00 a	45.00±0.00 a	30.00±0.00 a	40.00±0.00 a
Cast26	45.00±0.00 a	45.00±0.00 a	35.00±6.24 b	45.00±0.00 a
Curopos15	45.00±0.00 a	45.00±0.00 a	35.00±8.67 a	37.00±7.55 a
VBC02	45.00±0.00 a	45.00±0.00 a	20.00±0.00 b	45.00±0.00 a

In this study, the mycelial growth of all virulent isolates (VDP11, Cast13, Cast26, Curopos15, and VBC02) was observed to be uniform, with each isolate exhibiting a growth of 45.00 millimeters. This finding suggests that under non-converted conditions, there are no significant differences in the mycelial growth among these isolates.

Upon conversion by the factor SR44.2, all isolates continued to demonstrate similar mycelial growth, and no statistically significant differences were observed. This indicates that the application of SR44.2 did not have a discernible impact on the mycelial growth of the isolates. However, when converted by RBB111, a notable variation emerged. Cast26 and VBC02 exhibited a significant reduction in mycelial growth compared to the other isolates, suggesting that RBB111 has a distinct effect on these particular isolates.

Similarly, the conversion by Serra05 also resulted in a decrease of the mycelial growth for Curopos 15 and VDP 11, however, this diminution is not significative. Additionally, Cast26 displayed a lower growth, although the difference was not as pronounced as in the case of VBC02. These outcomes imply that the choice of conversion factor, specifically RBB111 and Serra05, can influence the mycelial growth of certain isolates, introducing variability that should be considered in the context of cultivation conditions.

VII.1.2.The *CHV-1* detection results

Results of RNA extraction were confirmed by visualizing the bands on agarose gel as shown in **Figure 16**. In fact, ORF A and ORF B used to identify the presence of the hypovirus *CHV-1* in total RNA extracted was identified in nearly all the converted strains. The hypothesis is confirmed and *CHV-1* was transferred to the virulent strains.

In fact, total intact RNA analyzed on agarose gel shows clear 28S and 18S rRNA bands. The detection of only one of the ORF, A or B is sufficient to confirm the *CHV-1* detection.

The results for all the strains of this work are illustrated in the **Table 5** which shows that the primers annealed and *CHV-1* was detected in nearly all of the strains, The result is negative for the strain VDP 11 interacting with RBB 111. This can be explained by the divergence of the *vic* type. In fact, VDP 11 and RBB 111 have different *vic* types EU 66 and EU 11, respectively but this doesn't explain why VDP 11 has been converted successfully with Serra 05 and SR44.2.

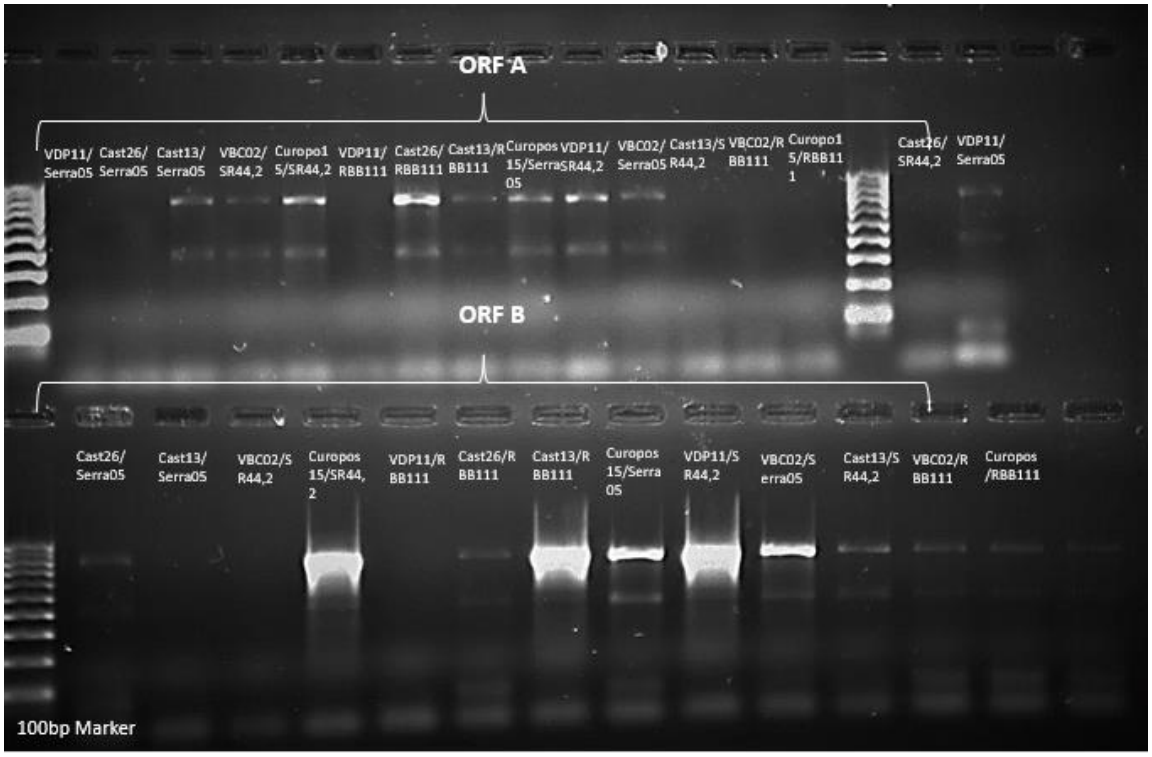

Figure 16 : *CHV-1* detection in total RNA extracted from converted strains.

Table 5: *CHV-1* primers detection on agarose gel results after total RNA extraction.

Converted strains	ORF A	ORF B	Results
Cast 26/SR44.2	Positive	Positive	Positive
VBC 02/SR44.2	Positive	Positive	Positive
VDP 11/SR44.2	Negative	Positive	Positive
Cast 13/SR44.2	Positive	Positive	Positive
Curopos 15/SR44.2	Positive	Negative	Positive
Cast 26/RBB 111	Positive	Negative	Positive
VBC 02/RBB 111	Positive	Positive	Positive
VDP 11/RBB 111	**Negative**	**Negative**	**Negative**
Cast 13/RBB 111	Positive	Positive	Positive
Curopos 15/RBB 111	Positive	Positive	Positive
Cast 26/Serra 05	Positive	Positive	Positive
VBC 02/Serra 05	Positive	Positive	Positive
VDP 11/Serra 05	Negative	Positive	Positive
Cast 13/Serra 05	Positive	Positive	Positive
Curopos 15/Serra 05	Positive	Negative	Positive

For work progression Curopos 15 (EU11) was the virulent strain chosen, as well as its three isogenic converted isolates with SR44.2, Serra 05 and RBB111, all EU11. In these isolates RNA was extracted again using both the TRIZOL method, and the plant Fungal Total RNA Purification Kit by Norgen Biotek Corp. In the case of this work, the extraction using the kit resulted in a better appearance of the two bands of S18 and S28 bands on agarose gel by electrophoresis, which leads us to conclude that the RNA was better extracted.

VII.2. RNA quantification results

The purity of the RNA extracted in confirmed when the OD_{260}/OD_{280} ratio is or between 1.8 and 2 or between 2 and 2.2. The values in the **Table 6** below confirms the purity of the RNA extracted from the four samples selected.

In the analysis of the extracted RNA from the four samples, it was observed that the A260/A280 ratio falls within the acceptable range (1.8 to 2 or 2 to 2.2) for all samples, affirming the purity of the RNA obtained.

The concentrations of calculated RNA ([RNA]) were determined and are expressed in µg/mL for each sample, reflecting reasonably high values. This suggests a favorable yield of RNA from the extraction process. In summary, the comprehensive results point towards the success of the RNA extraction procedure, demonstrating both acceptable purity and substantial RNA yield for the examined four samples.

Table 6 : RNA quantification and purity ratio**.**

Sample	**CUROPOS 15 / SR44.2**	**CUROPOS 15 / RBB 111**	**CUROPOS 15 / SERRA 05**	**CUROPOS 15**
Abs 260	0.1295	0.109	0.1195	0.1565
Abs 280	0.065	0.0595	0.0605	0.086
Dilution Factor	140	140.4	100.29	140
OD = 1 for RNA (µg/mL)	40	40	40	40
[RNA] (µg/mL)	725.2	612.14	479.37	876.4
Ratio A260/A280	2.0	1.8	2.0	1.8
RNA for 1000 ng/µL	1.4	1.6	2.1	1.1

VII.3. Verification results of the primers

The synthesis of the cDNA was performed using the protocol in **Appendix 5**.

To evaluate the primers, a series of PCR runs were conducted following the parameters outlined in the prescribed protocol in the **Appendix 6**. The initial sample of synthetized cDNA chosen involved Curopos 15, the virulent strain interacting with *CHV-1* by SR44.2. An initial test with OAH primers yielded inconclusive results, necessitating the design of an additional OAH primer for this study.

For the Rbsl_L5 primer, the thermal cycler program was optimized to improve the annealing. A temperature gradient (54°C, 56.8°C, and 59°C) was applied during the annealing phase using the program's thermal cycler. The outcome revealed the presence of a band at all three temperatures in the electrophoresis results, approximately 200bp according to the 100bp marker. Notably, the band intensity increased with higher temperatures, with optimal hybridization observed at 59°C.

To enhance the efficiency of GADP primer amplification, a series of new PCR experiments were conducted employing different annealing temperatures (56°C, 57°C, and 58°C) along

with an additional concentration of MgCl2. Gel electrophoresis was utilized using a 6X dye to analyze the resulting PCR products.

Electrophoresis revealed a distinct band consistently appearing between 100 and 200 base pairs across all tested annealing temperatures. Notably, the inclusion of extra MgCl2 contributed to the refinement of the reaction, facilitating the emergence of a single, well-defined band.

These experiments optimized conditions on the GADP primer specificity. The observed band within the 100 to 200 base pair range indicates a more targeted and desirable amplification.

Further optimization efforts may involve the annealing temperature within this range to pinpoint the exact temperature that maximizes the specificity and efficiency of the GADP primer. The success of these experiments establishes a foundation for more precise and reliable GADP primer-based PCR reactions in subsequent analyses.

These efforts in primer validation shows the critical importance of meticulous optimization, encompassing alternative primers design and reaction conditions adjustment. Such measures are essential to ensure the accuracy and specificity of subsequent molecular analyses.

VIII. Conclusion and perspective

In conclusion, this study examined the complex interaction between virulent strains and virulent strains infected with *CHV-1* of *Cryphonectria parasitica.* Through a comprehensive analysis of 15 cross cultures and meticulous phenotypic observations, virulent and hypovirulent strains grow at the same way on PDA, virulent strains may grow few millimeters more but this difference is not considered significative. After conversion, the orange color diminished until it disappeared as the culture medium was renewed, with the appearance of a white mycelium and a clear reduction in sporulation. These conversions could influence various aspects of the fungus's biology, including its virulence, tolerance to environmental conditions, and resistance to biological control agents (Milgroom and Cortesi, 2004).

The conversion process involving RBB111(EU11) and Serra05 (EU11) for transferring the *CHV-1* hypovirus has a notable impact on the mycelial growth of virulent isolates, leading to significant differences. Specifically, RBB111 causes a significant decrease in the growth of Cast 13 and VBC 02. Additionally, Serra05 significantly affects the growth of VBC 02 and has a somewhat lesser impact on Cast 26. On the other hand, other conversions, particularly those involving the hypovirulent strain SR44.2 (EU11), do not seem to have a significant effect on mycelial growth.

These findings collectively suggest that the interaction with *CHV-1* in virulent strains, especially through RBB111 and Serra 05, can selectively influence the growth of certain isolates highlighting the nuanced effects of hypovirus transfer.

Subsequent extraction of RNA from converted isolates cultures proved decisive in revealing genetic confirmation of the presence of the virus within the extracted total RNA.

In this particular study, the use of the total fungal RNA purification kit (Norgen Biotek Corp) and the TRIZOL method, revealed that the kit method was more efficient in extracting *C. parasitica* total RNA, thus providing a solid basis for subsequent molecular analysis.

We also verified that the optimization of PCR reactions by assaying MgCl2 concentration and gradient temperatures allowed us to improve the results of reaction when using the primers Rbs1_L5 and GADP. However, it is crucial to note that the primer designed for OAH did not provide the expected results. In response to this failure, an alternative primer was designed.

In the future, after get optimized OAH primers, real-time experiments could be used to evaluate the effect of the conversion of *C. parasitica* virulent strains in the attenuation of virulence measured by the decrease in *OAH* expression.

References

Anagnostakis, S.L., 1982. Genetic analysis of *Endothia parasitica*: linkage data for four single genes and three vegetative compatibility types. *Genetics* 102, 25–28. https://doi.org/10.1093/genetics/102.1.25.

Anagnostakis, S.L., 1986. Diversity of vegetative compatibility groups of *Cryphonectria parasitica* in Connecticut and Europe. *Plant Dis.* 70, 536. https://doi.org/10.1094/PD-70-536.

Argyropoulos, D.S., Menachem, S.B., 1997. Lignin, in: Eriksson, K.-E.L., Babel, W., Blanch, H.W., Cooney, Ch.L., Enfors, S.-O., Eriksson, K.-E.L., Fiechter, A., Klibanov, A.M., Mattiasson, B., Primrose, S.B., Rehm, H.J., Rogers, P.L., Sahm, H., Schügerl, K., Tsao, G.T., Venkat, K., Villadsen, J., Von Stockar, U., Wandrey, C. (Eds.), *Biotechnology in the Pulp and Paper Industry*, Advances in Biochemical Engineering/Biotechnology. Springer Berlin Heidelberg, Berlin, Heidelberg, pp. 127–158. https://doi.org/10.1007/BFb0102073.

Arnold, G.R.W., 1980. Barr, Margaret E., The diaporthales in North America with emphasis on *gnomonia* and its segregates. *Mycologia Memoir* No. 7. Published for the New York Botanical Garden in collaboration with the Mycological Society of America. 232 S. J. Cramer. Lehre, 1978. *Feddes Repert.* 91, 198–199. https://doi.org/10.1002/fedr.19800910313.

Bidlack, J., 1992. Molecular structure and component integration of secondary cell walls in plants.

Bragança, H., Simões, S., Onofre, N., Tenreiro, R., Rigling, D., 2007. *Cryphonectria parasitica* in Portugal: diversity of vegetative compatibility types, mating types, and occurrence of hypovirulence. *Forest Pathol.* 37, 391–402. https://doi.org/10.1111/j.1439-0329.2007.00513.

Bragança, H., Simões, S., Capelo, M., Marcelino, J., Santos, N., 2018. Survey and geographic distribution of chestnut blight in Portugal. *Revista de Ciências Agrárias* 148–158. https://doi.org/10.19084/RCA.15615.

Bryner, S.F., Rigling, D., Brunner, P.C., 2012. Invasion history and demographic pattern of *Cryphonectria hypovirus 1* across European populations of the chestnut blight fungus. *Ecol. Evol.* 2, 3227–3241. https://doi.org/10.1002/ece3.429.

Caten, C.E., 1972. Vegetative incompatibility and cytoplasmic infection in fungi. *J. Gen. Microbiol.* 72, 221–229. https://doi.org/10.1099/00221287-72-2-221.

Chen, C., Sun, Q., Narayanan, B., Nuss, D.L., Herzberg, O., 2010. Structure of oxalacetate acetylhydrolase, a virulence factor of the chestnut blight fungus. *J. Biol. Chem.* 285, 26685–26696. https://doi.org/10.1074/jbc.M110.117804.

Choi, G.H., Dawe, A.L., Churbanov, A., Smith, M.L., Milgroom, M.G., Nuss, D.L., 2012. Molecular characterization of vegetative incompatibility genes that restrict hypovirus transmission in the chestnut blight fungus *Cryphonectria parasitica*. *Genetics* 190, 113–127. https://doi.org/10.1534/genetics.111.133983.

Chun, J., Ko, Y.-H., Kim, D.-H., 2020. Transcriptome analysis of *Cryphonectria parasitica* infected with *Cryphonectria hypovirus 1* (CHV-1) reveals distinct genes related to fungal metabolites, virulence, antiviral RNA-silencing, and their regulation. *Front. Microbiol.* 11, 1711. https://doi.org/10.3389/fmicb.2020.01711.

Conedera, M., Krebs, P., Tinner, W., Pradella, M., Torriani, D., 2004. The cultivation of *Castanea sativa* (Mill.) in Europe, from its origin to its diffusion on a continental scale. *Veget. Hist. Archaeobot.* 13. https://doi.org/10.1007/s00334-004-0038-7.

Cortesi, P., McCulloch, C.E., Song, H., Lin, H., Milgroom, M.G., 2001. Genetic control of horizontal virus transmission in the chestnut blight fungus, *Cryphonectria parasitica*. *Genetics* 159, 107–118.

Cortesi, P., Milgroom, M.G., 1998. Genetics of vegetative incompatibility in *Cryphonectria parasitica*. *Appl. Environ. Microbiol.* 64, 2988–2994.

Cortesi, P., Rigling, D., Heiniger, U., 1998. Comparison of vegetative compatibility types in Italian and Swiss subpopulations of *Cryphonectria parasitica*. *Forest Pathol.* 28, 167–176. https://doi.org/10.1111/j.1439-0329.1998.tb01247.

Dutech, C., Barrès, B., Bridier, J., Robin, C., Milgroom, M.G., Ravigné, V., 2012. The chestnut blight fungus world tour: successive introduction events from diverse origins in an invasive plant fungal pathogen: world introduction of *Cryphonectria parasitica*. *Mol. Ecol.* 21, 3931–3946. https://doi.org/10.1111/j.1365-294X.2012.05575.

Fahima, T., Kazmierczak, P., Hansen, D.R., Pfeiffer, P., Van Alfen, N.K., 1993. Membrane-associated replication of an unencapsidated double-strand RNA of the fungus, *Cryphonectria parasitica*. *Virology* 195, 81–89. https://doi.org/10.1006/viro.1993.1348.

Feau, N., Dutech, C., Brusini, J., Rigling, D., Robin, C., 2014. Multiple introductions and recombination in *Cryphonectria hypovirus 1*: perspective for a sustainable biological control of chestnut blight. *Evol. Appl.* 7, 580–596. https://doi.org/10.1111/eva.12157.

Giangrande, M., Kim, Y.W., Mizukami, H., 1975. N-terminal spin label studies of hemoglobin, ligand and pH dependence. *Biochim. Biophys. Acta* 412, 187–193. https://doi.org/10.1016/0005-2795(75)90351-7.

Gilland, K.E., Keiffer, C.H., McCarthy, B.C., 2012. Seed production of mature forest-grown American chestnut (*Castanea dentata* (Marsh.) Borkh). *J. Torrey Bot. Soc.* 139, 283–289. https://doi.org/10.3159/TORREY-D-11-00071.1.

Gobbin, D., Hoegger, P.J., Heiniger, U., Rigling, D., 2003. Sequence variation and evolution of *Cryphonectria hypovirus 1* (CHV-1) in Europe. *Virus Res.* 97, 39–46. https://doi.org/10.1016/S0168-1702(03)00220.

Han, Y., Joosten, H.-J., Niu, W., Zhao, Z., Mariano, P.S., McCalman, M., Van Kan, J., Schaap, P.J., Dunaway-Mariano, D., 2007. Oxaloacetate hydrolase, the C–C bond lyase of oxalate secreting fungi. *J. Biol. Chem.* 282, 9581–9590. https://doi.org/10.1074/jbc.M611482200.

Havir, E.A., Anagnostakis, S.L., 1983. Oxalate production by *virulent but not by hypovirulent strains of *Endothia parasitica* (chestnut blight). *Physiol. Plant Pathol.* 23, 369–376. https://doi.org/10.1016/0048-4059(83)90055.

Havir, E.A., Anagnostakis, S.L., 1985. Oxalate accumulation by *virulent but not by hypovirulent strains of *Endothia parasitica* is influenced by growth medium. *Physiol. Plant Pathol.* 27, 369–376. https://doi.org/10.1016/0048-4059(85)90055.

Havir, E.A., Anagnostakis, S.L., 1984. Respiration during growth and conidiation of *virulent and hypovirulent strains of *Endothia parasitica*. *Physiol. Plant Pathol.* 24, 353–361. https://doi.org/10.1016/0048-4059(84)90055.

Havir, E.A., Wilcox, H.E., 1980. Chestnut blight: detection of isolates of *Endothia parasitica* with reduced virulence to American chestnut. *Phytopathology* 70, 968. https://doi.org/10.1094/Phyto-70-968.

Heiniger, U., Rigling, D., 1994. Biological control of chestnut blight in Europe. *Annu. Rev. Phytopathol.* 32, 581–599. https://doi.org/10.1146/annurev.py.32.090194.003053.

Hebard, F.V., 2012. The American Chestnut Foundation breeding program. *Annu. Rev. Phytopathol.* 50, 477–499. https://doi.org/10.1146/annurev-phyto-081211-173003.

Hebard, F.V., Griffin, G.J., Elkins, J.R., 1984. Developmental histopathology of cankers incited by hypovirulent and virulent isolates of *Endothia parasitica* on susceptible and resistant chestnut trees. *Phytopathology* 74, 140. https://doi.org/10.1094/Phyto-74-140.

Heinze, T. (Ed.), 2005. *Polysaccharides I: Structure, Characterisation and Use*, Advances in Polymer Science. Springer, Berlin; New York.

Kim, D.H., 1995. A new extracellular laccase of *Cryphonectria parasitica* is revealed by deletion of Lac1. *Mol. Plant Microbe Interact.* 8, 259. https://doi.org/10.1094/MPMI-8-0259.

Lei, L., Li, S., Gu, Y., 2012. Cellulose synthase complexes: composition and regulation. *Front. Plant Sci.* 3. https://doi.org/10.3389/fpls.2012.00075.

Ouni, O.A., Jorge, L., Moura, L., Coelho, V., Gouveia, E., 2020. Virulence, ligninolytic enzymes and metabolic profile of *Cryphonectria parasitica* virulent and hypovirulent strains converted by CHV-1 hypovirus. *Millenium* 2, 11–21. https://doi.org/10.29352/mill0213.01.00285.

Özkilinç, H., 2018. Ida dağı'nın yerel kestane ağaçlarındaki *Cryphonectria parasitica*'nın karakteriz. *AFGU* 35, 38–45. https://doi.org/10.13002/jafag4357.

Peever, T.L., Liu, Y.-C., Cortesi, P., Milgroom, M.G., 2000. Variation in tolerance and virulence in the chestnut blight fungus-hypovirus interaction. *Appl. Environ. Microbiol.* 66, 4863–4869. https://doi.org/10.1128/AEM.66.11.4863-4869.2000.

Piontek, K., Smith, A.T., Blodig, W., 2001. Lignin peroxidase structure and function. *Biochem. Soc. Trans.* 29, 111–116. https://doi.org/10.1042/bst0290111.

Prospero, S., Rigling, D., 2013. Chestnut blight., Gonthier, P., Nicolotti, G. (Eds.), *Infectious Forest Diseases*. CABI, UK, pp. 318–339. https://doi.org/10.1079/9781780640402.0318.

Rigling, D., Borst, N., Cornejo, C., Supatashvili, A., Prospero, S., 2018. Genetic and phenotypic characterization of *Cryphonectria hypovirus 1* from Eurasian Georgia. *Viruses* 10, 687. https://doi.org/10.3390/v10120687.

Rigling, D., Prospero, S., 2018. *Cryphonectria parasitica*, the causal agent of chestnut blight: invasion history, population biology and disease control: *Cryphonectria parasitica*. *Mol. Plant Pathol.* 19, 7–20. https://doi.org/10.1111/mpp.12542.

Rigling, D., Robin, C., Prospero, S., 2021. Mycovirus-mediated biological control, in: *Encyclopedia of Virology*. Elsevier, pp. 468–477. https://doi.org/10.1016/B978-0-12-809633-8.21516-1.

Robin, C., Anziani, C., Cortesi, P., 2000. Relationship between biological control, incidence of hypovirulence, and diversity of vegetative compatibility types of *Cryphonectria parasitica* in France. *Phytopathology* 90, 730–737. https://doi.org/10.1094/PHYTO.2000.90.7.730.

Robin, C., Heiniger, U., 2001. Chestnut blight in Europe: diversity of *Cryphonectria parasitica*, hypovirulence and biocontrol. *Forest Snow Landsc. Res.* 76, 361–367.

Savino, S., Bulgari, D., Monti, E., Gobbi, E., 2021. Agro-industrial wastes: a substrate for multi-enzymes production by *Cryphonectria parasitica*. *Fermentation* 7, 279. https://doi.org/10.3390/fermentation7040279.

Segers, G.C., Zhang, X., Deng, F., Sun, Q., Nuss, D.L., 2007. Evidence that RNA silencing functions as an antiviral defense mechanism in fungi. *Proc. Natl. Acad. Sci. U.S.A.* 104, 12902–12906. https://doi.org/10.1073/pnas.0702500104.

Appendix

1. RNA extraction by the TRIZOL method.

1. Weigh out 50-100mg of mycelium previously macerated with liquid N (it should be powdery) (no more than 10% of the volume of Trizol).
2. Add 1000µL of Trizol to the macerated mycelium in the Eppendorf.
3. Homogenize the sample with a blue and yellow tip and shake vigorously in a vortex; incubate at room temperature for 5 minutes for complete dilution.
4. Centrifuge at 12500g (11700rpm) for 10 minutes at 4ºC; (This additional centrifugation is advisable to remove polysaccharides (plant tissues or cellulose and chitin), proteins or other insoluble extracellular components; lipids accumulate in the upper layer). Remove the supernatant to a new tube.

At this stage, the samples can be stored in Trizol for one month at -60 to - 70ºC.

To use them, they should be allowed to thaw at room temperature or 5-10 minutes

1. Add 0.2 ml of chloroform for each ml of Trizol. Invert the tubes and shake vigorously by hand for 20 seconds. Incubate at 15-30ºC for 10 minutes, shaking periodically.
2. Centrifuge the samples at 11400 rpm for 15 minutes at 4ºC.
3. Transfer the aqueous phase (top, about 60 percent of the initial volume of Trizol collect ~40 percent) to a new tube without touching the interface.
4. Add 0.5ml of isopropanol per ml of Trizol. Invert the tubes and incubate for 15 minutes at room temperature; centrifuge at 12000g for 10 minutes at 4ºC (for RNA extractions, you should not see the ball, as it is DNA).

OR

1. Add 0.25ml of isopropanol and 0.25ml of a high-salt precipitation solution (0.8M sodium citrate; 1.2M NaCl) per ml of Trizol. Shake vigorously before incubation at room T° for 10 minutes. The centrifugation at 12000g for 10 minutes at 4ºC. In this case, polysaccharides and proteoglycans remain in the soluble phase, separating from the RNA.
2. Remove the supernatant and keep only the pellet.
3. Wash the pellet with 1ml of 75% ethanol with ice-cold DEPC. Pour off the pellet, pipette, and vortex. Centrifuge at 7000rpm (7500g) for 5 or 10 minutes at 4ºC (orientate the tubes in the microcentrifuge to better locate the "pellet.".

4. Discard the supernatant carefully. Do not leave the tube inverted or lying down; remove excess ethanol with a tip, if necessary, after a spin - and air dry the pellet for 5-10 minutes (do not let it dry completely).

At this stage, the precipitate can be stored in 75% ethanol for one week at 2-8ºC or one year at -5 to -20ºC.

5. Resuspend the pellet in 20µL of water with DEPC (10 µL if there is little pellet). Pipette. To better solubilize the pellet, place it in an oven at 55-60ºC for 10 minutes and pipette again and store at -70ºC or -20ºC.

Place 3 µL of the sample plus 3 µL of blue - 2x RNA loading dye - in an Eppendorf for5 minutes at 70ºC.

Chomczynski P and Sacchi N, Single-step method of RNA
isolationby acid guanidinium thiocyanate-phenol-chloroform
extraction, Analbiochem 162, 156-159 (1987)

2. Protocol for *CHV-1* virus detection

A - RNA extraction

The Plant Fungal Total RNA Purification kit (Norgen Biotek Corp) is used for RNA extraction.

1. Collect 40 mg of lyophilized mycelium and add 600 µL of Lysis Buffer (144 µL of β-Mercaptoethanol + 14.4 ml of Lysis Buffer, which must be put together previously). Vortex for 20 s. Centrifuge 2 minutes at 14,000 rpm.
2. Transfer the supernatant to a new tube (RNASE-free tube). Add the same volume of 100% ethanol to the tube. Mix by vortexing.
1. Transfer 600 µL of the solution into a new kit tube (spin columns). Centrifuge 1 minute At 14,000 rpm. (Repeat if necessary).
1. Discard the supernatant in a new tube with column (spin columns). Add 400 µL Wash Solution to the column. Centrifuge 2 minutes at 14,000 rpm.
2. Discard the supernatant and add 400 µL of Wash Solution—centrifuge for 1 minute at 14,000 rpm.
3. Discard the supernatant and add 400 µL of Wash Solution—centrifuge for 1 minute at 14,000 rpm.
4. Discard the supernatant and centrifuge for 2 minutes at 14,000 rpm without adding any solution (to dry the column).
5. Transfer the column into a new 1.7 ml tube from the kit.
6. Add 50 µL of Elution Buffer to the column. Centrifuge for two minutes at 2000 rpm and centrifuge again for seconds at 14000 rpm.
7. Discard the column and store the tube (- 4ºC).

Electrophoresis: 1.0% agarose gel, 80 V (3 µL of sample + 1 µL of blue dye + 2 µL of water U.P.) in TBE buffer. Marker 1Kb. Run 1 hour.

B - *CHV-1 identification*

For the identification of the *CHV-1* virus, RNA that has been previously extracted is used.

Step 1 : RNA dilution :

1. Centrifuge the RNA at 11,000 rpm for 4 minutes at room temperature. Make a dilution of the RNA, using microtubes, where 3 µL of Total RNA are placed, and 11 µL of Water Nuclease -free (Thermo Fisher Scientific Baltics UAB, Vilnius, Lithuania) are added (total of 14 µL). Vortex a few seconds before going to the thermal cycler.
2. Place the microtube thermocycler model T100 Thermal Cycler Bio-Rad at 100ºC for 2 minutes.

Step 2: Digestion: obtaining the complementary DNA (cDNA) (notes from Isabel Ibañez):

PCR reagents	**Quantity**
5x reaction mix	4 µL
Maxima Engyne mix	2 µL
Diluted RNA	14 µL
Total	**20 µL**

1) Perform a PCR to obtain the complementary DNA (cDNA) under the following conditions: 1 cycle (1X) consisting of denaturation at 95ºC for 10 minutes, ringing at 50ºC for 30 minutes and extension at 85ºC for 5 minutes, 10ºC infinite, in a thermal cycler model T100 Thermal Cycler (Bio-Rad).

Thermal cycler conditions. T= 47m :30s

Temperature	**Time**	**Cycles**
25ºC	10 minutes	1
50 ºC	30 minutes	
85 ºC	5 minutes	
10 ºC	infinity	

Step 3 - PCR amplification of the ORF region

2) Perform a PCR to observe the virus genome amplifying the ORF A and ORF B region using primer pairs:

3) Virus genome PCR (notes by Isabel Ibañez):

	Volume 20 µL		**Volume 50 µL**	
PCR reagent	**Quantity 1X**	**10X**	**Quantity 1X**	**10X**
Primer ORF A **hvep1F** (20 pmol/ µL)	0.5 µL	5 µL	1 µL	10 µL
Primer ORF A **EP721 -4** Rev (20 pmol/ µL)	0.5 µL)	5 µL	1 µL)	10 µL
Jump Star Red Taq 2x	10 µL	100 µL	10 µL	100 µL
cDNA	1 µL	-	1 µL	-
H2O	8 µL	80 µL	37 µL	370 µL
Total	**20 µL**	**(19+1) µL**	**50 µL**	**(49+1) µL**

4) A negative control (no RNA) is used in each PCR to detect any contamination.

for the ORF A region

ORF A Rev (5'- GGAAGTCGGACATGCCCTG - 3')

ORF A For (5`- TGACACGGAAGCTGAGTGTC - 3')

for the ORF B region

ORF B -12aF For (5'- AGACCTCAATCGGTCTCCCT - 3')

ORF B -12aR Rev (5'- TTCAACCACGACGAGTTCG - 3')

PCR is performed in a thermal cycler model T100 Thermal Cycler (Bio-Rad), starting with the initial denaturation at **94ºC for 2 minutes,** followed by 33 cycles consisting of denaturation at **94ºC for** seconds annealing at **55ºC for 90 seconds** and next extension at **72ºC for 2 minutes**. Finalized with **72ºC** for **8 minutes** is included to complete the incomplete PCR fragments, and in the extension process, 10ºC infinite. A negative control (without RNA) is used in each PCR to detect any contamination.

Thermal cycler conditions:

	Temperature	Time	Cycles
Initial denaturing	94ºC	2 minutes	1
Denaturalisation	94ºC	1 minute	33
Ringing	55 ºC	90 seconds	
Extension	72 ºC	2 minutes	
Final extension	72 ºC	8 minutes	1

VIRUS ORF programme, T= ±3h :15m

5) Display of PCR products.

Electrophoresis: 1.5% agarose gel in TBE buffer (60 ml TBE, 0.9 gr agarose, 1.2 µL gel red), 80 V (4 µL of sample+1 µL of blue dye + 1 µL P.U. water). Use as molecular marker 100 bp DNA Marker (Bioron).

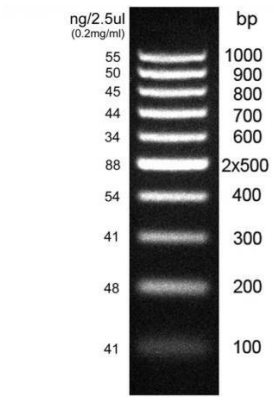

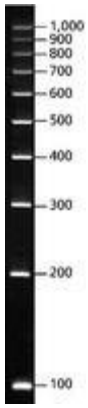

100 bp DNA Marker **PCR 100 bp low lader (sigma)**

3. 2X RNA loading dye solution

This solution is recommended for the preparation of RiboRuler^{TM} RNA ladders and RNA samples for electrophoresis on agarose or polyacrylamide gels. It contains electrophoresis tracking dyes; bromophenol blue, xylene cyanol FF, and the intercalating dye ethidium bromide. In most denaturing agarose gel systems, bromophenol blue migrates slightly faster than human 5S rRNA, whereas xylene cyanol FF migrates slightly slower than 18S rRNA. Fermentas 2X RNA loading Dye Solution contains the denaturing agent formamide, thus in most cases RNA molecules are separated according to their size even during non-denaturing electrophoresis. In addition, formamide stabilizes RNA.

Composition:

95% formamide
0.025% SDS
0.025% bromophenol blue
0.025% xylene cyanol FF
0.025% ethidium bromide
0.5mM EDTA

Storage:

Store at room temperature or at +4°C for periods up 12 months.
For longer periods, store at -20°C.

4. cDNA synthesis

The iScript Select cDNA Synthesis Kit.

The cDNA synthesis kit supplied all necessary reagents, excluding the RNA template and gene-specific primers, essential for generating first-strand cDNA from an RNA template. All kit components are optimized to streamline the process of cDNA synthesis, accommodating input total RNA ranging from 1 pg to 1 µg for efficient results.

The iScript Reverse Transcriptase comprises a recombinant RNase H+ Moloney murine leukemia virus (MMLV) reverse transcriptase, preblended with a recombinant RNase inhibitor. Its activity is fine-tuned for compatibility with the 5x iScript Select Reaction Mix. This reaction mix is a distinctive combination of buffers, stabilizers, and dNTPs, simplifying the reaction setup and guaranteeing the robust synthesis of first-strand cDNA. Moreover, this kit's potent enzyme and exclusive buffer formulation work in tandem to minimize error rates during the cDNA synthesis process.

The iScript Select cDNA Synthesis Kit enhances the priming of the first strand by incorporating a proprietary enhancer solution during the primer-template hybridization step. This enhancer is preblended with the oligo(dT) primers and random primers supplied in the kit, simplifying the reaction setup. As a result, there is no need to separately add the enhancer solution to reactions that use the provided primer mixes. However, when utilizing a gene-specific primer (GSP), it is necessary to include the enhancer solution in the reaction. A distinct protocol and tube labeled GSP enhancer solution are included for this specific purpose. Including the enhancer solution in cDNA reactions can significantly enhance yields, leading to earlier detection in real-time PCR.

Storage and Stability

Store at –20°C. Guaranteed for 12 months at –20°C in a constant temperature freezer. Nuclease-free water can be stored at room temperature

Reaction Setup with Gene-Specific Primers

Place components on ice after a vortex

1) Add the following components

Components	Volume per Reaction (µL)
5x iScript Select Reaction Mix	4

iScript enzyme (reverse-transcriptase)	1
Gene-specific primer (2–10 pmol)	Variable (100-500 nM in 20µL final volume)
GSP enhancer solution	2
RNA template (1 pg–1 µg total RNA)	Variable
Nuclease-free water	Variable
Total volume	20

1. Incubate first at 42°C for 10–60 min.
2. Incubate at 85°C for 5 min for the inactivation of the reverse transcriptase.
3. Store cDNA product at -20 to 4°C.
4. The resulting cDNA product is ready for amplification. One-tenth of the first-strand reaction typically provides a sufficient target for most PCR applications.

Optionally, the cDNA can be diluted in Tris-EDTA buffer (10 mM Tris [pH 8.0], 0.1 mM EDTA) to add larger volumes to PCR reactions.

5. Bioron DFS-Taq DNA polymerase protocol

Applications: DFS-Taq DNA Polymerase is suitable for all regular applications PCR, primer extension reactions etc. DFS-Taq is free of bacterial DNA and therefore suitable for detection of pathogen bacteria. DFS-Taq DNA Polymerase effectively directs PCR with templates up to 5 kb in length.

Sensitivity: detection of ≥ 10 DNA molecules

Additionally provided: 1 tube $MgCl_2$ (100 mM)

Recommended $MgCl_2$ concentration: 1.5 mM – 6 mM

Storage condition: -20 °C

Pipetting scheme and thermocycler protocol

Components	**Volume / 50 µL Reaction**	**Final concentration**
10 x PCR-Buffer	5 µL	1 x
dNTP-Mix (10 mM each)	1 µL	200 µM each
Upstream Primer	variable	0.1 - 0.5 µM
Downstream Primer	variable	0.1 - 0.5 µM
DFS-Taq DNA Polymerasee	0.25 - 1.0 µL	1.25 - 5.0 units
Template DNA	variable	10 to 500 ng/reaction
Sterile dest. water	Adjust to 50 µL final volume	

Separate $MgCl_2$ solution can be used for optimization.

Thermocycle protocol

step	**time**	**temperature**
initial denaturation	3 minutes	94 °C
37 cycles		
denaturation	30 seconds	94 °C
annealing	20 seconds	55 - 68 °C *
extension	1 minute	72 °C

Usually, the optimal annealing temperature is 5 °C below the melting temperature of the primers.